

RESEARCH ARTICLE

Pharmacological and genetic activation of cAMP synthesis disrupts cholesterol utilization in *Mycobacterium tuberculosis*

Kaley M. Wilburn¹, Christine R. Montague¹, Bo Qin², Ashley K. Woods², Melissa S. Love², Case W. McNamara², Peter G. Schultz², Teresa L. Southard³, Lu Huang¹, H. Michael Petrassi², Brian C. VanderVen^{1*}

1 Microbiology & Immunology, Cornell University, Ithaca, New York, United States of America, **2** Calibr, a division of The Scripps Research Institute, San Diego, California, United States of America, **3** Biomedical Sciences, Cornell University, Ithaca, New York, United States of America

* bcv8@cornell.edu



OPEN ACCESS

Citation: Wilburn KM, Montague CR, Qin B, Woods AK, Love MS, McNamara CW, et al. (2022) Pharmacological and genetic activation of cAMP synthesis disrupts cholesterol utilization in *Mycobacterium tuberculosis*. PLoS Pathog 18(2): e1009862. <https://doi.org/10.1371/journal.ppat.1009862>

Editor: Christopher M. Sassetti, University of Massachusetts Medical School, UNITED STATES

Received: July 29, 2021

Accepted: January 18, 2022

Published: February 8, 2022

Copyright: © 2022 Wilburn et al. This is an open access article distributed under the terms of the [Creative Commons Attribution License](https://creativecommons.org/licenses/by/4.0/), which permits unrestricted use, distribution, and reproduction in any medium, provided the original author and source are credited.

Data Availability Statement: With the exception of unprocessed RNA-seq data files, all relevant data can be found within the manuscript and its [Supporting Information](#) files. All RNA-seq dataset files are available at NCBI GenBank, at <https://www.ncbi.nlm.nih.gov/geo/query/acc.cgi?acc=GSE190875>.

Funding: This work was supported by grants #AI130018 and #AI119122 from the National Institute of Allergy and Infectious Diseases (<https://www.nih.gov/>)

Abstract

There is a growing appreciation for the idea that bacterial utilization of host-derived lipids, including cholesterol, supports *Mycobacterium tuberculosis* (Mtb) pathogenesis. This has generated interest in identifying novel antibiotics that can disrupt cholesterol utilization by Mtb *in vivo*. Here we identify a novel small molecule agonist (V-59) of the Mtb adenylyl cyclase Rv1625c, which stimulates 3', 5'-cyclic adenosine monophosphate (cAMP) synthesis and inhibits cholesterol utilization by Mtb. Similarly, using a complementary genetic approach that induces bacterial cAMP synthesis independent of Rv1625c, we demonstrate that inducing cAMP synthesis is sufficient to inhibit cholesterol utilization in Mtb. Although the physiological roles of individual adenylyl cyclase enzymes in Mtb are largely unknown, here we demonstrate that the transmembrane region of Rv1625c is required during cholesterol metabolism. Finally, the pharmacokinetic properties of Rv1625c agonists have been optimized, producing an orally-available Rv1625c agonist that impairs Mtb pathogenesis in infected mice. Collectively, this work demonstrates a role for Rv1625c and cAMP signaling in controlling cholesterol metabolism in Mtb and establishes that cAMP signaling can be pharmacologically manipulated for the development of new antibiotic strategies.

Author summary

The recalcitrance of *Mycobacterium tuberculosis* (Mtb) to conventional antibiotics has created a need to identify novel pharmacological mechanisms to inhibit Mtb pathogenesis. There is a growing understanding of the metabolic adaptations Mtb adopts during infection to support its survival and pathogenesis. This has generated interest in identifying small molecule compounds that effectively inhibit these *in vivo* metabolic adaptations, while overcoming challenges like poor pharmacokinetic properties or redundancy in target pathways. The Mtb cholesterol utilization pathway has repeatedly been speculated to be a desirable antibiotic target, but compounds that successfully inhibit this complex

www.niaid.nih.gov/) to B.V. and grants #OPP1107194 and #OPP1208899 from the Bill & Melinda Gates Foundation (<https://www.gatesfoundation.org/>) to Calibr at Scripps Research. The funders had no role in study design, data collection and analysis, decision to publish, or preparation of the manuscript.

Competing interests: The authors have declared that no competing interests exist.

pathway and are suitable for use *in vivo* are lacking. Here, we establish that stimulating cAMP synthesis in Mtb is a mechanism that is sufficient to block cholesterol utilization by the bacterium, preventing the release of key metabolic intermediates that are derived from breakdown of the cholesterol molecule. This work also identifies small molecule agonists of the Mtb adenylyl cyclase Rv1625c that have promising pharmacological properties and are suitable for use during *in vivo* studies. These Rv1625c agonists increase cAMP synthesis, inhibit cholesterol utilization by Mtb, and disrupt Mtb pathogenesis in mouse models of chronic infection.

Introduction

Tuberculosis (TB) remains a prevalent infectious disease worldwide that claims ~1.4 million lives and afflicts ~10 million new individuals annually [1]. TB is caused by *Mycobacterium tuberculosis* (Mtb), and it is an ongoing challenge to identify antibiotics with novel bacterial targets that can shorten treatment, limit side-effects, and reduce disease relapse. An important aspect of Mtb pathogenesis is that the bacterium persists in the human lung within lipid-rich phagocytes and/or tissue lesions while promoting pathology that is required for dissemination and transmission [2]. Mtb primarily lives within macrophages and stimulates the formation of lipid-loaded cells [3,4], but the bacterium can also survive in the acellular core of necrotic granulomas that are rich in cholesterol, cholesterol ester, and triacylglycerols [2,5]. It is generally understood that Mtb utilizes host-derived lipids, including cholesterol, as key nutrients to survive during persistent infection [6]. Mtb completely degrades cholesterol into two- and three-carbon intermediates that are metabolized for energy production or serve as biosynthetic precursors of cell wall or virulence lipids [6]. In animal models, Mtb requires cholesterol metabolism to maintain optimal chronic lung infection [7–11] and cholesterol utilization was recently found to belong to a set of “core virulence functions” required for Mtb survival *in vivo* across a genetically diverse panel of mice [12]. Furthermore, it was recently demonstrated that a multi-drug resistant strain of Mtb is more dependent on cholesterol for growth than the H37Rv reference strain [13]. Thus, cholesterol metabolism in Mtb represents a novel, genetically validated target for drug discovery. However, tools to pharmacologically inhibit this pathway during infection *in vivo* have yet to be developed.

Signaling through the universal second-messenger 3',5'-cyclic adenosine monophosphate (cAMP) has long been studied in a variety of prokaryotic and eukaryotic systems. In pathogenic bacteria, cAMP is essential in regulating functions such as carbon metabolism, virulence gene expression, biofilm formation, drug tolerance, and manipulation of host cell signaling [14–16]. How cAMP signaling regulates Mtb physiology during infection is not well understood, partly due to the limited tools available for investigating this and the myriad of pathway components present in Mtb. The Mtb genome encodes an unusually large repertoire of at least ten biochemically active class III adenylyl cyclase (AC) enzymes, which catalyze the intramolecular cyclization of ATP to form cAMP upon activation. These ACs are structurally diverse, and the majority of these proteins are composed of a catalytic domain along with other accessory domains, which are thought to participate in regulatory or effector functions [17]. Studies using recombinant expression systems have proposed environmental stimuli (e.g. pH, fatty acids, or CO₂) for five Mtb ACs [18–22]. Additionally, Mtb possesses twelve predicted downstream cAMP-binding effector proteins, only four of which have been functionally characterized [23–28]. Thus, our understanding of how individual ACs and downstream cAMP-dependent effector proteins regulate specific aspects of Mtb physiology is extremely limited.

To date, no individual AC enzyme has been directly linked to the regulation of a specific biological or metabolic process in Mtb.

We previously identified a series of compounds that inhibit Mtb growth in macrophages and in cholesterol media [29]. The activity of a subset of these compounds is dependent on the AC Rv1625c, and compound treatment increased cAMP production in Mtb [29]. The Rv1625c protein is composed of at least four structural elements: an N-terminal cytoplasmic tail, a six-helical transmembrane domain, a cytoplasmic helical domain, and a C-terminal cyclase domain. Based on its topology and sequence homology, Rv1625c is comparable to ‘one-half’ of a mammalian membrane-associated AC [30]. Rv1625c forms a homodimer to generate two active sites composed of complementary residues, and conserved active site residues as well as the cytoplasmic tail and helical domain have been linked to its catalytic activity [31–33]. Although it has been proposed that Rv1625c may be activated by binding CO₂ or lipophilic ligands, it remains unclear what the native role of Rv1625c is in Mtb during infection [19,34,35]. The possibility that we had identified chemical tools comparable to forskolin in the Mtb system led us to investigate the mechanism of these Rv1625c-dependent compounds and their impact on Mtb carbon metabolism and pathogenesis. We were especially motivated to test the hypothesis that activating cAMP synthesis in Mtb through an Rv1625c agonist could disable cholesterol utilization and undermine Mtb persistence during infection in mice.

To carry out these studies, we re-examined our previously identified screening hits for Rv1625c-dependent compounds with favorable pharmacokinetic properties. From these, we selected a potent compound (V-59) that permitted both *in vitro* and *in vivo* studies to examine the impact that chemically activating cAMP signaling has on Mtb metabolism. In this work, we determined that V-59 is an Rv1625c agonist, and its ability to inhibit Mtb growth in macrophages and cholesterol is dependent on Rv1625c and an associated increase in cAMP synthesis. Additionally, we found that the transmembrane domain of Rv1625c is necessary for the complete metabolism of cholesterol, linking the protein target of V-59 directly to the cholesterol utilization pathway. This finding connects a single AC to the regulation of a downstream metabolic pathway in Mtb. Using a complementary genetic approach, we developed an inducible system to activate cAMP synthesis independent of V-59 and Rv1625c, and determined that upregulating cAMP synthesis is sufficient to inhibit cholesterol utilization in Mtb. V-59 was optimized through medicinal chemistry, which produced a lead compound (mCLB073) with improved potency and *in vivo* activity against Mtb when delivered orally to infected mice. Collectively, our results reveal a novel cAMP signaling mechanism in Mtb that inhibits cholesterol utilization and may represent an improvement over developing conventional single-step inhibitors against this complex pathway. Using a small molecule AC agonist as an antimicrobial compound is an unconventional approach, and this study explores this as a mechanism of action to inhibit growth of a bacterial pathogen during infection.

Results

V-59 inhibits Mtb growth and requires Rv1625c for activity

We previously identified compounds that inhibit Mtb replication in macrophages (29) and determined that one of these compounds (V-58) preferentially inhibits Mtb growth in cholesterol media in an Rv1625c dependent manner [36]. Unfortunately, these previously identified compounds have poor potency and pharmacological properties. For example, a resynthesized analog of V-58 (sCEB942) displayed sub-optimal intramacrophage potency that could not be improved (S1 Table). Similarly, the previously identified compound (mCCY224) displayed poor solubility, high plasma protein binding, and high levels of caseum binding (S1 Table). These properties precluded the use of these Rv1625c-dependent compounds in mice. Since a

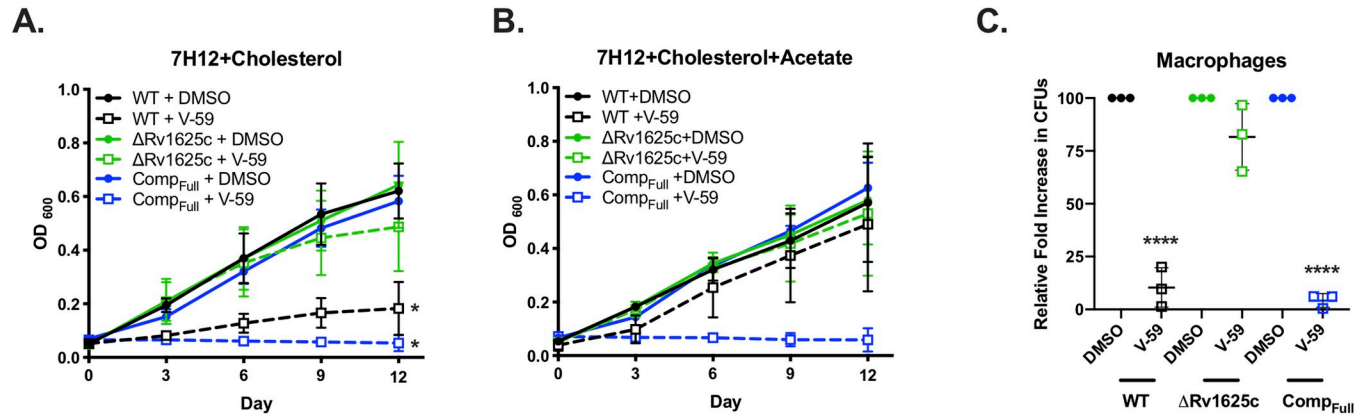


Fig 1. V-59 inhibits Mtb growth in an Rv1625c-dependent mechanism. (A and B) Impact of V-59 on Mtb growth in cholesterol media (A) and in media containing cholesterol and acetate (B). V-59 (10 μ M) was added to the cultures every three days, and DMSO is the vehicle control. Data are from two experiments, with three technical replicates each (* P < 0.05, One-way ANOVA with Sidak's multiple comparisons test). (C) Effect of V-59 on growth of Mtb in murine macrophages. Macrophages were infected at an MOI of 2 and treated with V-59 (25 μ M) or DMSO. Data are from three experiments with two or more technical replicates each (**** P < 0.0001, One-way ANOVA with Sidak's multiple comparisons test on fold-change in CFUs normalized to DMSO). All data are means \pm SD.

<https://doi.org/10.1371/journal.ppat.1009862.g001>

primary goal of this work was to investigate the impact that activating cAMP synthesis has on Mtb physiology during infection in mice, we re-examined our screening hits to identify candidate Rv1625c-dependent compounds with more favorable pharmacological properties that are permissible for both *in vivo* and *in vitro* studies. This effort revealed a small molecule 1-(4-(5-(4-fluorophenyl)-2H-tetrazol-2-yl)piperidin-1-yl)-2-(4-methyl-1,2,5-oxadiazol-3-yl)ethan-1-one, named V-59, that inhibits Mtb replication in macrophages (half maximal effective concentration (EC₅₀) 0.30 μ M). Because the availability of carbon sources can potentially impact activity of chemical inhibitors against Mtb, V-59 was evaluated in different *in vitro* culture conditions. Similar to a previously characterized Rv1625c agonist [36], V-59 inhibits Mtb growth in cholesterol media (EC₅₀ 0.70 μ M) (Figs 1A and 2) but not in media containing the two-carbon fatty acid acetate, or in standard rich growth media (Figs 1B and 2). V-59 also displayed a promising pharmacokinetic profile (Fig 2) and was therefore selected for further investigation as a potential Rv1625c agonist.

V-59 is structurally distinct from previous cholesterol utilization inhibitor candidates (S1 Table). Similar to a subset of other cholesterol-dependent Mtb growth inhibitors we identified [29], a transposon insertion in the *rv1625c* gene (Tn::*rv1625c*) confers resistance to V-59 (S1A Fig). Inversely, WT Mtb transformed with an *rv1625c* overexpression plasmid (2x*rv1625c*) was ~15-fold more susceptible to V-59 than WT (S1A Fig). This heightened susceptibility suggests a mechanism in which V-59 activates Rv1625c, and growth inhibition scales with Rv1625c enzyme levels. To test this further, we deleted the gene encoding Rv1625c (Δ Rv1625c) and complemented this mutation with the entire *rv1625c* gene (Comp_{Full}). The Δ Rv1625c mutant is refractory to V-59 inhibition in cholesterol media (Figs 1A and S1B). Because macrophages contain various nutrients that can support Mtb growth [37] we determined that V-59 inhibits Mtb growth in murine macrophages *in vitro* and confirmed that Rv1625c is required for V-59 activity during macrophage infection (Figs 1C and S1C). Importantly, the Δ Rv1625c strain does not have a pan-drug resistance profile (S1D Fig). Across all of these assays, the Comp_{Full} strain was more susceptible to V-59 treatment relative to WT, even in media containing acetate. This is likely because *rv1625c* is overexpressed in the Comp_{Full} strain relative to its native expression levels in WT (S1E Fig). We conclude that a functional Rv1625c enzyme is required for V-59 activity, and that this compound inhibits Mtb growth in cholesterol media and macrophages.

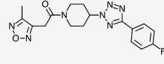
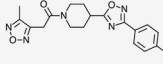
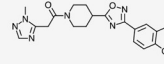
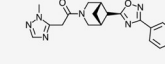
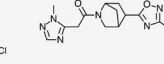
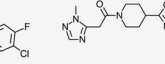
	Screen hit		Advanced leads			Optimized lead
	V-59	mCIS635	mCLE299	mCLF177	mCLF178	mCLB073
Subseries	Furazan	Furazan	Triazole	Triazole	Triazole	Triazole
						
MW	371.36	371.36	404.82	398.84	416.83	421.28
<i>In vitro</i> potency assays						
Macrophages EC ₅₀ (μM)	0.3	0.27	--	0.13	>20	1.2
Cholesterol EC ₅₀ (nM)	700	150	115	83	83	27
7H9 OADC EC ₅₀ (μM)	>50	>50	--	>50	>50	>50
Cholesterol/acetate EC ₅₀ (μM)	>50	>50	--	--	--	>50
Toxicity						
HepG2/HEK293 CC ₅₀ (μM)	>20/>20	>20/>20	25/40	>20/>20	>20/>20	>20/>20
hERG IC ₅₀ (μM)	8.9	9.5	22.3	26.3	22.9	13.8
ADME						
PPB mouse/human (% bound)	82.7/--	94.4/--	86.3/90.3	91.7/91.4	88.4/88.9	96.3/97.6
Caseum binding (% unbound)	--	2.65	--	3.1	1.7	1.2
Cyp IC ₅₀ (μM)	>30	>50	>50	>50	>30	>50
ER mouse/human/rat/dog	0.3/0.3/--	0.4/0.3/--	0.3/0.3/0.2/0.3	0.3/0.3/0.2/0.3	0.3/0.3/0.2/0.3	0.3/0.3/0.2/0.3
Solubility (μM, pH 6.8)	4.63	34.4	196.8	197.7	185.9	160.1
Time over EC ₅₀ (20 mg/kg PO)	24 hr	>23 hr	>24 hr	>24 hr	>24 hr	>24 hr

Fig 2. Structures and activities of compounds. MW, molecular weight; --, not determined; EC₅₀, half-maximal effective concentration; CC₅₀, 50% cytotoxic concentration; hERG, human ether-à-go-go-related gene; IC₅₀, half-maximal inhibitory concentration; ADME, absorption, distribution, metabolism, excretion; PPB, plasma protein binding; Cyp, cytochrome P450; ER, extraction ratio; PO, per oral.

<https://doi.org/10.1371/journal.ppat.1009862.g002>

Rv1625c is necessary and sufficient for V-59 to stimulate cAMP production

Rv1625c is a biochemically confirmed AC enzyme that catalyzes the intramolecular cyclization of ATP into cAMP [30]. Therefore, we determined whether V-59 increases cAMP production in whole bacteria in an Rv1625c-dependent manner. V-59 induced cAMP by ~70-fold in WT and ~140-fold in Comp_{Full}, but did not affect the ΔRv1625c mutant (Fig 3A). To determine whether Rv1625c is sufficient for V-59 to stimulate cAMP production, we heterologously expressed the *rv1625c* gene in an AC-deficient strain of *E. coli*. This strain is deficient in its own single AC (*cya*⁻ *E. coli*), ensuring that the cAMP produced in this experiment is due to Rv1625c activity [36]. V-59 treatment increased cAMP levels in *cya*⁻ *E. coli* transformed with the Rv1625c expression plasmid (Fig 3B). Similar results were obtained during treatment with an optimized analog of V-59, named mCLB073, which is described later in more detail. In Mtb, we found that spontaneous mutations in *rv1625c* confer resistance to V-59 (Fig 3C). Mutations predicted to truncate the Rv1625c protein and inactivate its cyclase domain resulted in resistance (S2A Fig). We also identified missense mutations within the transmembrane and cyclase domains of Rv1625c that confer resistance; without further biochemical characterization, it is ambiguous whether these mutations generate resistance by preventing V-59 binding to Rv1625c, or by disabling Rv1625c enzyme activity. Together these results indicate that V-59 activates Rv1625c selectively in Mtb, and that Rv1625c expression is sufficient for V-59 to activate cAMP synthesis, which is necessary for V-59 to inhibit Mtb growth.

Rv1625c is directly linked to cholesterol degradation in Mtb

Because V-59 impairs growth of Mtb in cholesterol media, we tested whether using V-59 to chemically activate Rv1625c inhibits the bacterium's ability to break down cholesterol. When Mtb degrades the A-ring of [4-¹⁴C]-cholesterol, [1-¹⁴C]-pyruvate is released; subsequently,

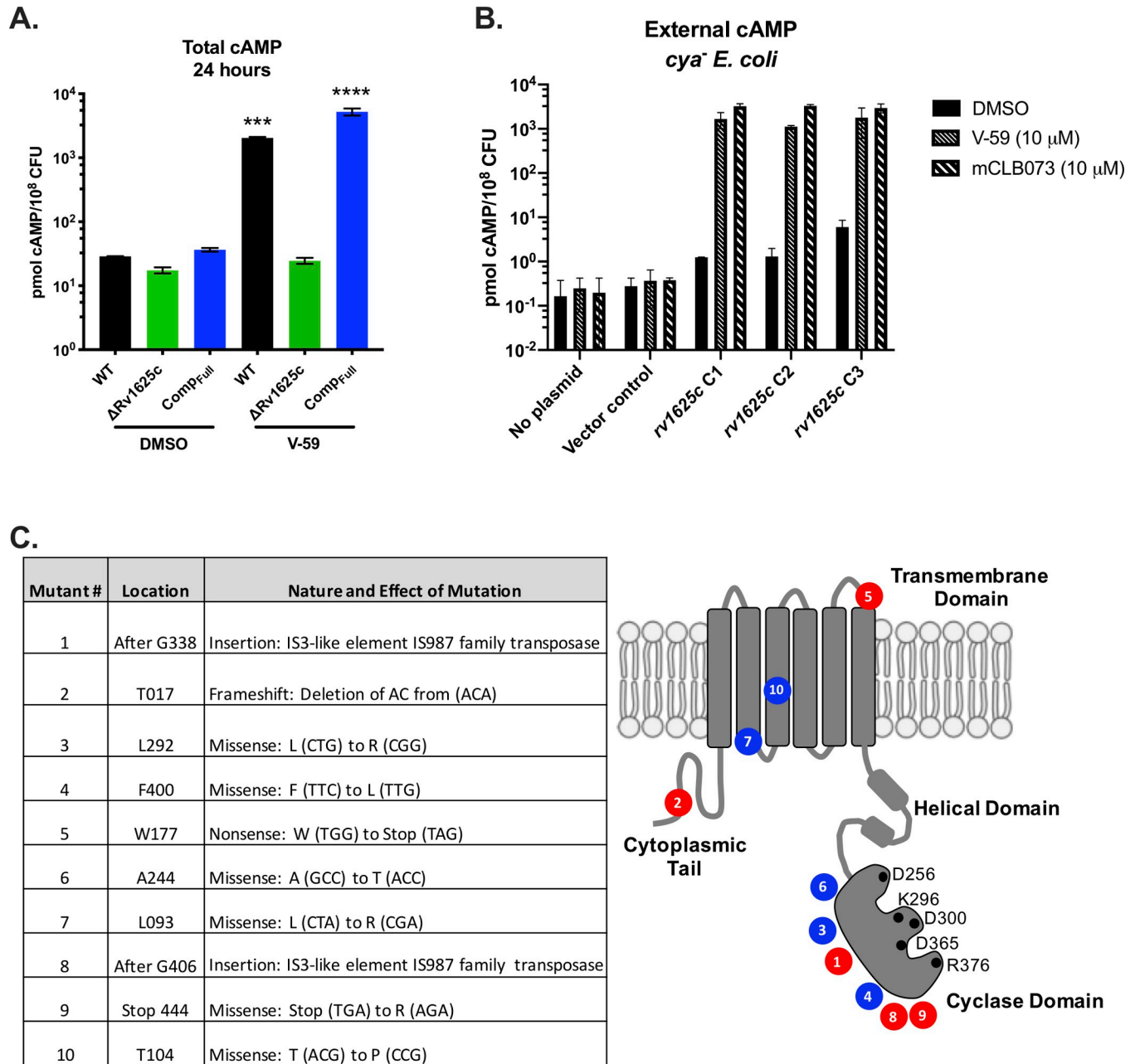


Fig 3. V-59 stimulates Rv1625c to produce cAMP. (A) Impact of V-59 on cAMP production in Mtb. Cultures were treated with V-59 or DMSO for 24 hours. Data are from two experiments with two technical replicates each (***P* < 0.001, *****P* < 0.0001, One-way ANOVA with Sidak's multiple comparisons test). (B) Impact of Rv1625c agonists on cAMP production in *cya*⁻ *E. coli* transformed with an empty vector control or an Rv1625c expression plasmid. Supernatants were collected 18 hours after addition of V-59, mCLB073, or DMSO. Data is from one experiment, with three independent expression clones, and two technical replicates each. In (A) and (B) Data are normalized as total cAMP per 10⁸ bacteria. DMSO is the vehicle control. Data are shown as means ± SD. (C) Summary of mutations in the *rv1625c* gene that confer resistance to Rv1625c agonists. Mutations are grouped by their effect on the *rv1625c* sequence, with missense mutations (blue) and insertion or frameshift mutations (red) and mapped on the Rv1625c topology diagram to illustrate their approximate location relative to Rv1625c protein domains. Black circles represent amino acids that are essential for AC activity.

<https://doi.org/10.1371/journal.ppat.1009862.g003>

pyruvate dehydrogenase activity mediates the conversion of [1-¹⁴C]-pyruvate into acetyl-CoA and ¹⁴CO₂ [6]. Therefore, to quantify cholesterol degradation in Mtb, we captured ¹⁴CO₂ released following [4-¹⁴C]-cholesterol breakdown by the bacteria [38]. We found that V-59

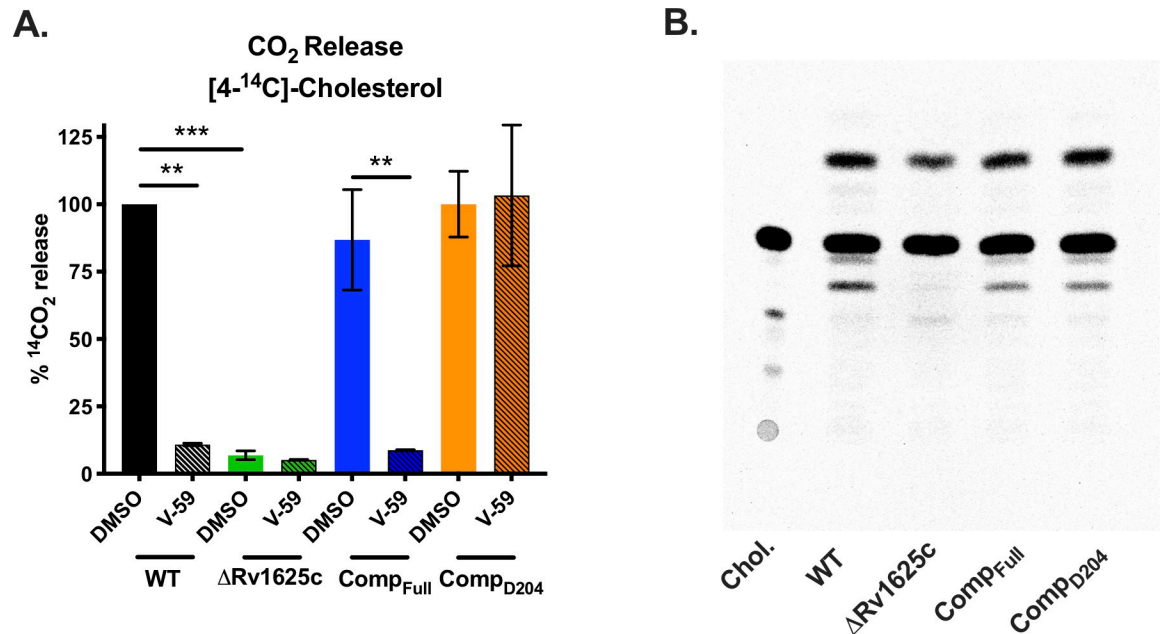


Fig 4. The transmembrane domain of Rv1625c is essential for complete degradation of cholesterol and the catalytic domain of Rv1625c is required for V-59 activity. (A) Catabolic release of ¹⁴CO₂ from [4-¹⁴C]-cholesterol in WT, ΔRv1625c, Comp_{Full}, and Comp_{D204} strains treated with V-59 (10 μM) or DMSO vehicle control. Data are from two experiments with three technical replicates, normalized to OD and quantified relative to WT treated with DMSO. Shown as means ± SD (***P* < 0.01, ****P* < 0.001, Two-way ANOVA with Tukey's multiple comparisons test). (B) TLC comparing [4-¹⁴C]-cholesterol-derived metabolites extracted from supernatants of Mtb. Image is representative of two experiments. Equivalent counts were spotted per lane. "Chol." = [4-¹⁴C]-cholesterol.

<https://doi.org/10.1371/journal.ppat.1009862.g004>

decreased ¹⁴CO₂ release in WT by ~89% (Fig 4A). By contrast, V-59 had no measurable effect on ¹⁴CO₂ released from breakdown of the fatty acid [U-¹⁴C]-palmitate (S3A Fig). This suggests that chemically activating Rv1625c preferentially inhibits cholesterol utilization in WT Mtb, rather than equally inhibiting all lipid utilization by the bacterium.

Unexpectedly, we found that the ΔRv1625c mutant has an intrinsic defect in cholesterol degradation (Fig 4A). In contrast to ΔRv1625c, the Rv1625c transposon mutant strain (Tn::*rv1625c*) had no defect in ¹⁴CO₂ release from [4-¹⁴C]-cholesterol (S3B Fig). The Tn::*rv1625c* strain has a transposon insertion within the coding sequence located after the last exit of Rv1625c's six-helical transmembrane domain (amino acid Y302) (S3C Fig). This likely truncates the protein, eliminating more than half of the C-terminal cyclase domain, while leaving the N-terminal cytoplasmic tail and six-helical transmembrane domain intact. Thus, we complemented the ΔRv1625c strain with a construct that expresses only the N-terminal cytoplasmic tail and six-helical transmembrane domain of Rv1625c (Comp_{D204}) (S3C Fig). Cholesterol degradation was restored in the Comp_{D204} strain (Fig 4A), indicating that the transmembrane domain of Rv1625c is required for the complete degradation of cholesterol. Importantly, V-59 inhibited ¹⁴CO₂ release in the Comp_{Full} strain; however, V-59 did not prevent ¹⁴CO₂ release in the Comp_{D204} strain which lacks the Rv1625c cyclase domain (Fig 4A).

To further examine whether cholesterol degradation is blocked in ΔRv1625c Mtb, we used thin-layer chromatography (TLC) to track accumulation of [4-¹⁴C]-cholesterol-derived metabolites. Compared to WT Mtb, the culture supernatant of ΔRv1625c was deficient in at least one cholesterol-derived degradation intermediate, and the production of this intermediate was restored in the Comp_{Full} strain (Fig 4B). Collectively, these results indicate that the cyclase domain of Rv1625c must be present for V-59 to inhibit cholesterol catabolism, and the

transmembrane domain of Rv1625c is required for complete cholesterol breakdown, thereby establishing a direct link between the target of V-59 and the cholesterol pathway in Mtb. To our knowledge, this is the first AC that has been linked to modulation of a downstream metabolic pathway in Mtb.

Inducing cAMP synthesis is sufficient to regulate cholesterol utilization

Next, we investigated whether cAMP signaling can modulate cholesterol metabolism in an Rv1625c-independent manner by using a novel inducible construct (TetOn-cAMP) to increase cAMP synthesis in Mtb. This TetOn-cAMP construct carries an anhydrotetracycline (Atc) inducible promoter that controls expression of the catalytic domain of the mycobacterial AC Rv1264 [18] (S4A Fig). Atc induced cAMP synthesis in WT Mtb carrying the TetOn-cAMP construct in a dose-dependent manner, reaching levels comparable with V-59 treatment (Fig 5A). This tool is an advancement over previous approaches [24,39] for several reasons: it does not rely on diffusion of an external cAMP analog into the bacteria, it requires the bacteria to synthesize cAMP from ATP which more closely models the dynamics of AC signaling, and it increases cAMP by 24 hours post-induction in a dose-dependent fashion. Atc treatment inhibited growth of WT bacteria carrying the TetOn-cAMP construct in cholesterol media (Fig 5B) and also decreased [4-¹⁴C]-cholesterol degradation to ¹⁴CO₂ (Fig 5C). Similar to V-59 treatment, activating cAMP synthesis with Atc did not inhibit degradation of the fatty acid [U-¹⁴C]-palmitate to ¹⁴CO₂ (S3A Fig). As a control, we modified the TetOn-cAMP construct by mutating a catalytic residue of Rv1264 (TetOn-Rv1264_{D265A}) to render it catalytically inactive [18]. Atc induced expression of the Rv1264_{D265A} protein in WT Mtb carrying the TetOn-Rv1264_{D265A} construct (S4B Fig), but this strain did not produce increased cAMP in response to Atc (S4C Fig). Inducing Rv1264_{D265A} expression did not inhibit bacterial growth in cholesterol media (S4D Fig) or cholesterol degradation (S4E and S4F Fig). These results demonstrate that activating cAMP synthesis through a mechanism that is independent of Rv1625c is sufficient to regulate cholesterol utilization in Mtb in a dose-dependent manner.

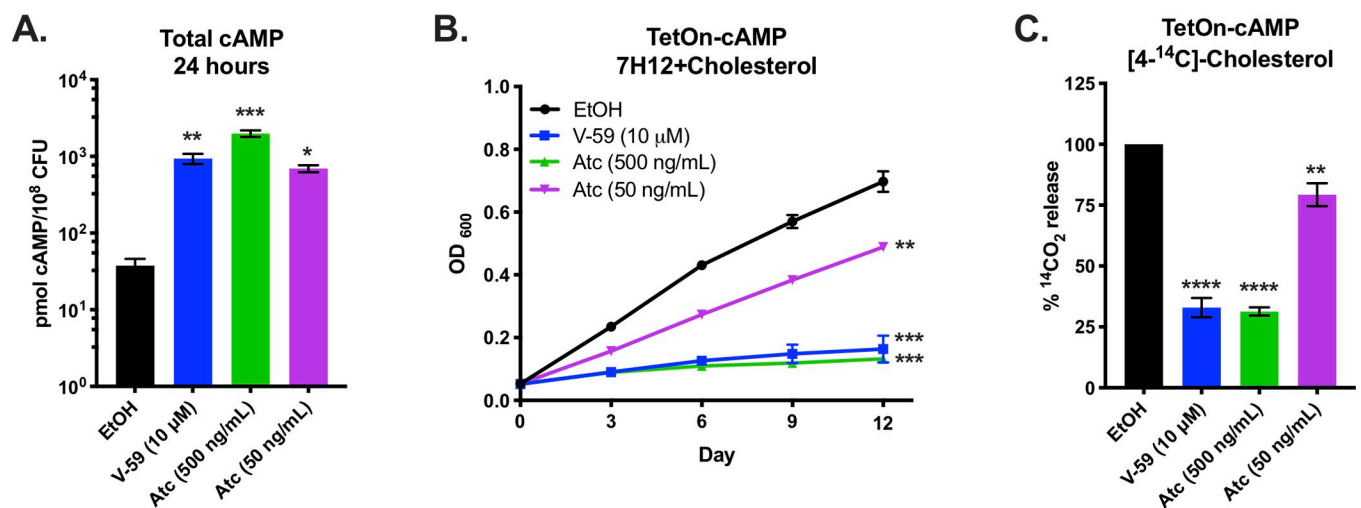


Fig 5. Inducing cAMP synthesis independent of V-59 and Rv1625c is sufficient to block cholesterol utilization. (A) Total cAMP induced in TetOn-cAMP Mtb. Cultures were treated with V-59 (10 μM), Atc (500 ng/mL or 50 ng/mL), or EtOH and samples were collected after 24 hours. Data are normalized as total cAMP per 10⁸ Mtb and are from two experiments with two technical replicates each. (B) Impact of inducing TetOn-cAMP on the growth of Mtb in cholesterol media. Cultures were treated with V-59 (10 μM) or Atc for the duration of the experiment. Data are from two experiments with three technical replicates. (C) Catabolic release of ¹⁴CO₂ from [4-¹⁴C]-cholesterol in the TetOn-cAMP strain treated with V-59, Atc, or EtOH. Data are from two experiments with three technical replicates, normalized to OD and quantified relative to EtOH EtOH is the vehicle control throughout. All data are means ± SD (**P* < 0.05, ***P* < 0.01, ****P* < 0.001, *****P* < 0.0001, One-way ANOVA with Dunnet's multiple comparisons test).

<https://doi.org/10.1371/journal.ppat.1009862.g005>

Common transcriptional changes in cholesterol genes are associated with cAMP induction

Next, we characterized transcriptional responses of Mtb following V-59 treatment, or upon induction of the TetOn-cAMP construct, during growth in cholesterol media. The RNA-seq datasets revealed a shared pattern of differential gene expression that is consistent with an early blockade in the cholesterol degradation pathway. In Mtb, the side-chain and A-B rings of cholesterol are degraded by enzymes encoded in the Rv3574/KstR1 regulon [6]. KstR1 is a TetR-like transcriptional repressor that binds the second cholesterol degradation intermediate, 3-hydroxy-cholest-5-ene-26-oyl-CoA, which de-represses the KstR1 regulon and permits cholesterol degradation to occur. Thus, increased expression of the KstR1 regulon is an indicator of cholesterol degradation in Mtb. Inducing cAMP synthesis, with V-59 or by activating TetOn-cAMP, prevented transcriptional induction of the KstR1 regulon in WT Mtb (Fig 6). This included key genes required for cholesterol transport (*rv0655/mceG* and *rv3502/yrbE4B*) and cholesterol catabolism [6]. Cholesterol degradation releases propionyl-CoA, and Mtb primarily assimilates this intermediate into central metabolism via the methylcitrate cycle (MCC) [6]. As propionyl-CoA pools increase, Mtb upregulates expression of the genes encoding MCC enzymes (*rv0467/icl1*, *rv1130/prpD*, *rv1131/prpC*) [40]. V-59 treatment and induction of the TetOn-cAMP construct in WT Mtb each prevented upregulation of MCC genes (Fig 6). Paralleling previous experiments, V-59 induced more pronounced changes in the transcriptional signature in the Comp_{Full} strain. Notably, genes required for cholesterol transport and genes (*hsaEFG*) necessary for conversion of the cholesterol-derived catabolic intermediate 2-hydroxy-hexa-2,4-dienoic acid to pyruvate and propionyl-CoA were upregulated in the Comp_{Full} strain following V-59 treatment [6]. It is plausible that these expression profiles reflect a compensatory response to inhibition of cholesterol degradation by V-59, and a concomitant decrease in availability of MCC or tricarboxylic acid cycle intermediates. Consistent with our previous observations (Fig 4), expression of cholesterol side-chain and ring degradation genes, but not transport or MCC genes, was intrinsically blocked in the Δ Rv1625c strain relative to WT (Fig 6). These observations further support the conclusion that Rv1625c is involved in downstream cholesterol metabolism in Mtb. Importantly, V-59 treatment did not alter the transcriptional signature of the Δ Rv1625c strain.

To validate these findings, we used a reporter (*prpD*::GFP) that expresses GFP under control of a MCC gene promoter (*prpD*), which indicates cellular levels of propionyl-CoA [38]. V-59 decreased GFP signal in WT by ~50%, but did not impact the Δ Rv1625c or Comp_{D204} strains in cholesterol media or during macrophage infection (Fig 7A). V-59 also dampened GFP signal by ~90% in the Comp_{Full} strain (Fig 7A). Similarly, inducing cAMP synthesis in WT Mtb carrying the TetOn-cAMP construct was sufficient to inhibit GFP signal during growth in cholesterol media and during macrophage infection (Fig 7B). Inducing expression of the inactive Rv1264_{D265A} protein (S4B Fig) did not change the GFP signal (S4F Fig). Overall, these data demonstrate that inducing cAMP synthesis in Mtb, via V-59 treatment or TetOn-cAMP activation, impairs cholesterol degradation and the release of key metabolic intermediates including propionyl-CoA in Mtb. During macrophage infection, additional signals not present in cholesterol media (e.g. low pH, additional carbon sources) that can regulate Mtb metabolism may also influence propionyl-CoA levels, contributing to overall *prpD*::GFP expression [41,42]. Importantly, the effects of V-59 treatment require the catalytic domain of Rv1625c, and cAMP synthesis is a dominant signal in the mechanism by which V-59 inhibits Mtb growth.

Mt-Pat is not required to mediate inhibition of cholesterol utilization

Inducing cAMP synthesis blocks cholesterol utilization in Mtb, but the mechanism mediating this is unknown. Because fatty acid metabolism can be modulated by the cAMP-binding

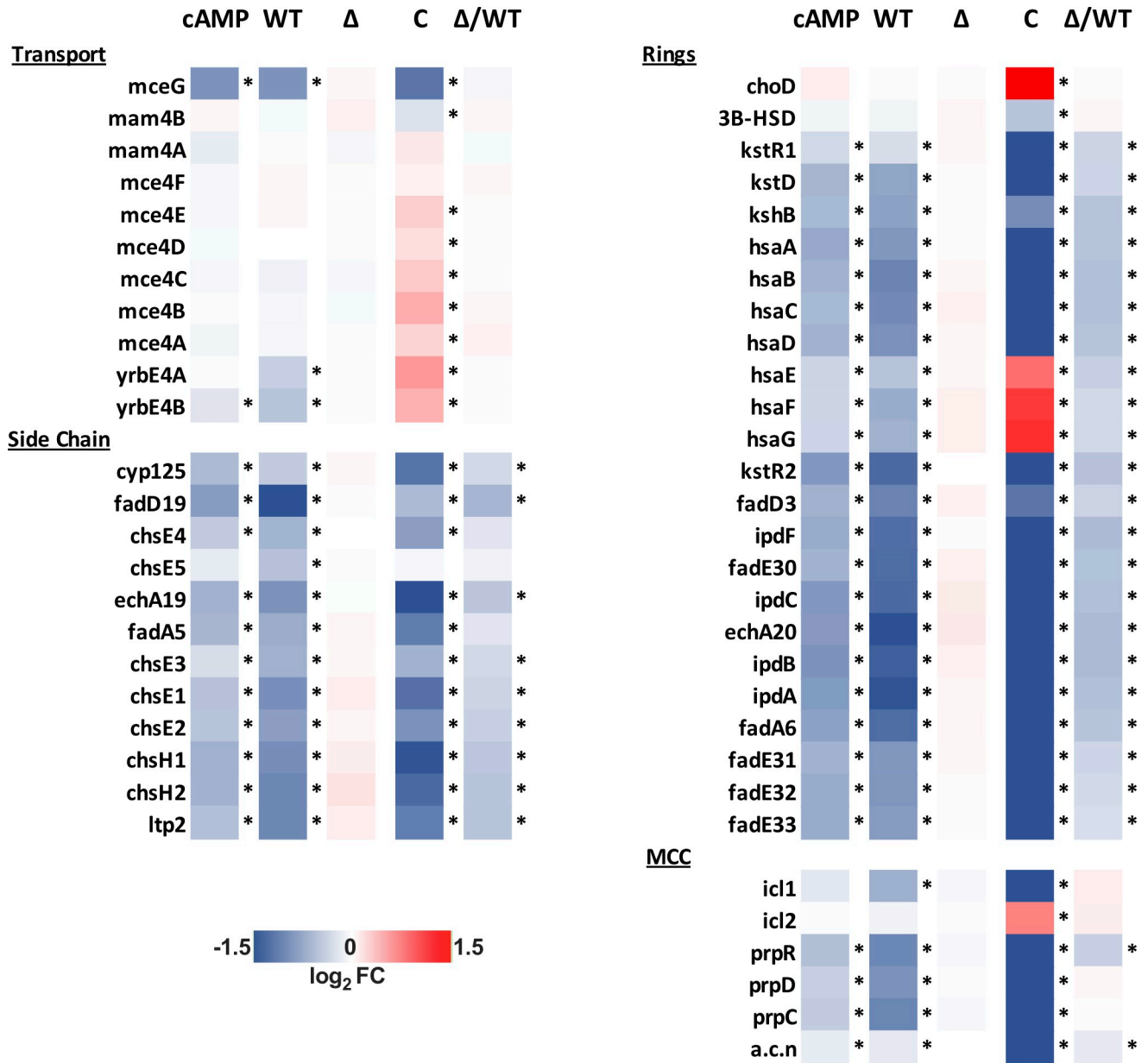


Fig 6. V-59 treatment and induction of TetOn-cAMP are associated with shared transcriptional changes to cholesterol utilization genes. RNA-seq analysis quantifying differentially expressed genes from Mtb grown in cholesterol media, following V-59 treatment, or induction of TetOn-cAMP with Atc. Genes depicted are in the KstR regulons and involved in cholesterol utilization. MCC = methylcitrate cycle. Data are displayed as log₂ fold change in gene expression in response to cAMP-inducing vs. control treatment (“cAMP” = Tet-On cAMP Atc vs. EtOH, “WT” = WT V-59 vs. DMSO, “Δ” = ΔRv1625 V-59 vs. DMSO, “C” = Comp_{Full} V-59 vs. DMSO). Also shown are differentially expressed genes intrinsic to ΔRv1625 (“Δ/WT” = ΔRv1625 DMSO vs. WT DMSO). Data are from two technical replicate samples from one experiment (* adjusted P-value ≤ 0.05).

<https://doi.org/10.1371/journal.ppat.1009862.g006>

protein Rv0998/Mt-Pat [27,28] we investigated whether Mt-Pat also mediates V-59-dependent inhibition of cholesterol utilization. However, inhibition of growth (S5A Fig) and inhibition of MCC gene induction (S5B Fig) by V-59 treatment were not altered in an Mt-Pat mutant. Notably, the Comp_{Full} strain was uniquely susceptible to V-59 in cholesterol media supplemented with the short chain fatty acid acetate (Figs 1B and S5C), and V-59 was also found to block MCC gene induction in the Comp_{Full} strain during growth with odd-chain fatty acids

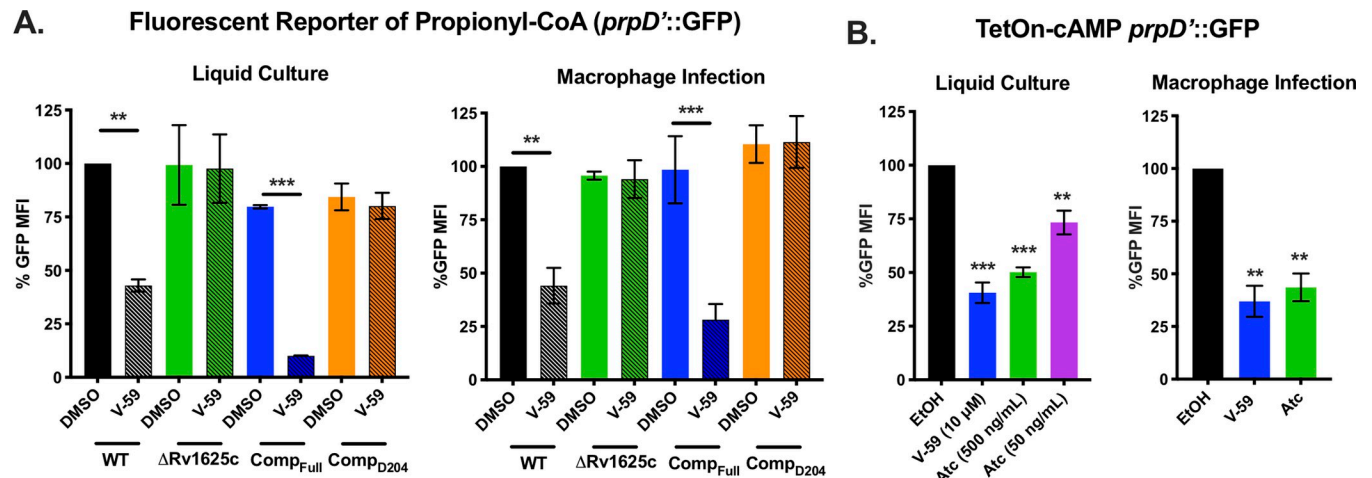


Fig 7. Activating cAMP synthesis decreases liberation of propionyl-CoA from cholesterol. (A) Relative GFP signal from the *prpD*::GFP reporter in response to V-59 (10 μM) or DMSO treatment in murine macrophages or cholesterol media. Data are normalized to WT treated with DMSO (** $P < 0.01$, *** $P < 0.001$, Two-way ANOVA with Tukey's multiple comparisons test). (B) Relative GFP signal from the *prpD*::GFP reporter in response to inducing TetOn-cAMP with Atc treatment in murine macrophages or cholesterol media. Data are normalized to EtOH vehicle control (** $P < 0.01$, *** $P < 0.001$, One-way ANOVA with Dunnett's multiple comparisons test). GFP MFI was quantified from 10,000 mCherry⁺ Mtb. Data are from two experiments with two technical replicates, shown as means ± SD.

<https://doi.org/10.1371/journal.ppat.1009862.g007>

(S5D Fig). This suggests that additional metabolic defects, possibly in fatty acid utilization or central metabolism, are induced under these conditions. While these observations correlate with a higher threshold of cAMP induction (Fig 3A), we have not determined whether Mt-Pat mediates these additional effects. In the future, identifying the pathway by which inducing cAMP synthesis modulates cholesterol catabolism in Mtb may explain the differing effects of V-59 on carbon metabolism in these strains.

Transcriptional changes in select CRP_{MT} regulon genes are associated with cAMP induction

To define a set of commonly regulated cAMP-dependent genes using an unbiased analysis, we compared all of the statistically significant differentially expressed genes associated with V-59 treatment or TetOn-cAMP induction in WT Mtb (Fig 8A). A shared set of 248 genes were identified (Fig 8B). Because the selected growth condition was cholesterol media, 45 of these genes are associated with cholesterol utilization. As discussed above, those with biochemically confirmed roles in cholesterol utilization were noted (Fig 6). Many of the remaining 203 genes do not have well defined functions in Mtb, and we chose to focus on a small subset that were previously predicted to be regulated by the cAMP-binding transcription factor Rv3676/CRP_{MT}.

Aside from Mt-Pat, CRP_{MT} is the best-studied cAMP-binding effector protein in Mtb. CRP_{MT} is designated as a potential cAMP-responsive transcription factor, with a predicted regulon of ~100 genes in Mtb [25,26,43]. CRP_{MT} may also be required to maintain Mtb fitness in macrophages and during chronic infection in mice [26]. We found that activating cAMP via V-59 treatment or TetOn-cAMP induction was associated with transcriptional changes to a shared set of only 9 CRP_{MT} regulon genes during growth in cholesterol media, which have unknown functions except for *rv0450c/mmpL4* and *rv0451c/mmpS4* (Fig 8C) [44]. Importantly, among the predicted CRP_{MT} regulon genes, *rv0805* is upregulated during V-59 treatment. Rv0805 is the only known phosphodiesterase in Mtb, and these enzymes contribute to

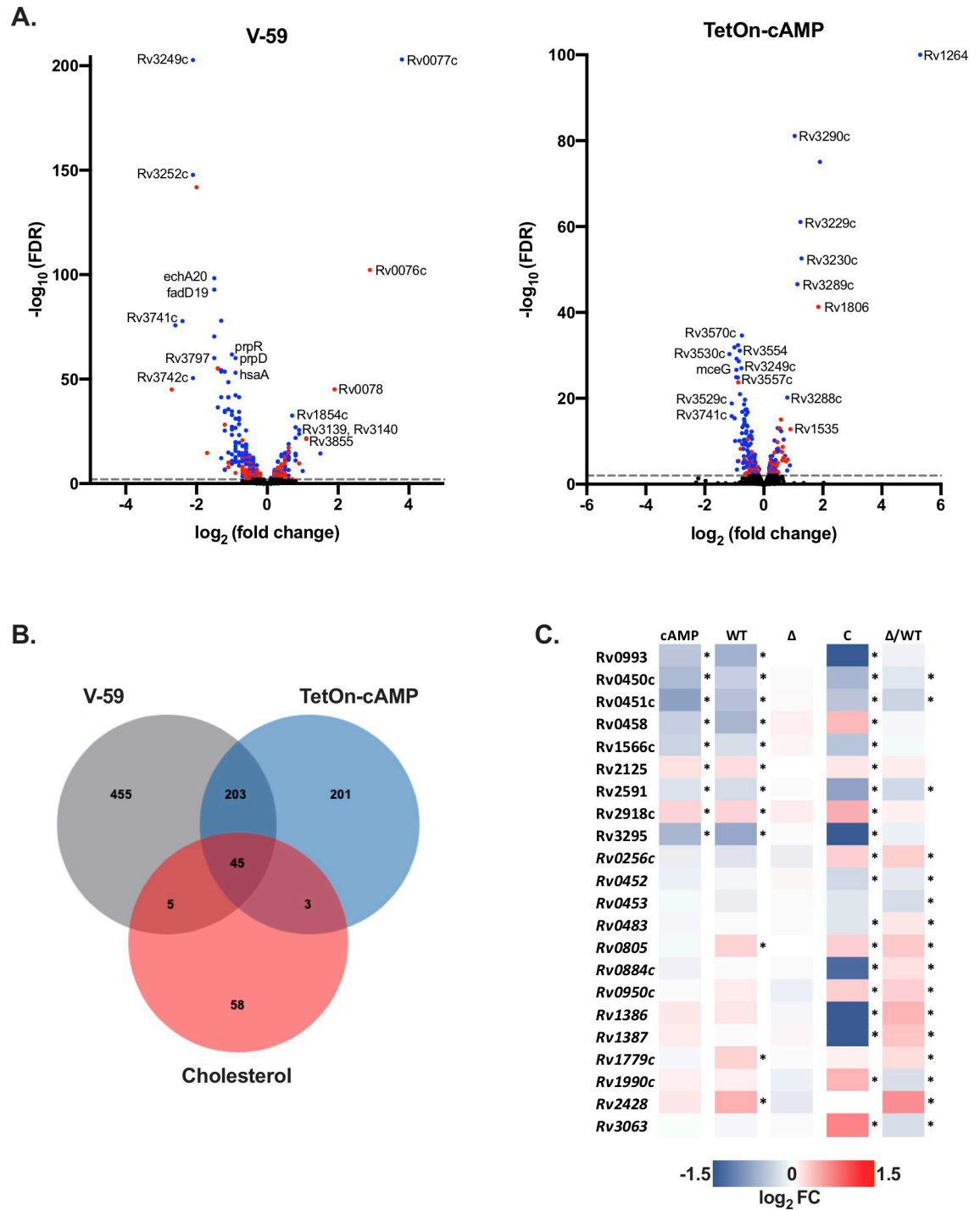


Fig 8. V-59 treatment and induction of TetOn-cAMP are associated with transcriptional changes in select CRP_{MT} regulon genes. (A) Volcano plots displaying differentially expressed genes following V-59 treatment of WT Mtb relative to DMSO control (left), or following Atc treatment of TetOn-cAMP Mtb relative to EtOH control (right), based on RNA-seq. Each dot represents a single gene, genes in blue are significant (FDR < 0.05) in both data sets and genes in red are unique to their respective data set. Dashed line indicates FDR cutoff < 0.01. (B) Venn diagram showing the number of significantly differentially expressed genes shared by the V-59 and TetOn-cAMP conditions, and how many of these belong to the KstR cholesterol-related regulon. (C) RNA-seq analysis quantifying differentially expressed genes from Mtb grown in cholesterol media, following V-59 treatment, or induction of TetOn-cAMP with Atc. Genes depicted are predicted members of the CRP_{MT} regulon. Only genes with significant differential expression in both the V-59 and TetOn-cAMP conditions, or genes with intrinsic changes in the ΔRv1625 strain (in italics), are shown. “cAMP” = Tet-On cAMP Atc vs. EtOH, “WT” = WT V-59 vs. DMSO, “Δ” = ΔRv1625 V-59 vs. DMSO, “C” = Comp_{Full} V-59 vs. DMSO, “Δ/WT” = ΔRv1625 DMSO vs. WT DMSO.

<https://doi.org/10.1371/journal.ppat.1009862.g008>

cAMP signaling pathway homeostasis by hydrolyzing cAMP to AMP [23]. Given that *rv0805* mutant Mtb also has a growth defect in cholesterol media [45], it is reasonable to speculate that *rv0805* is upregulated during V-59 treatment in the presence of cholesterol as a compensatory response to help decrease cAMP levels and restore cholesterol utilization. Taken together, this is consistent with our other results indicating that a threshold of increased cAMP is inhibitory during cholesterol utilization in Mtb. Surprisingly, an additional set of 13 predicted CRP_{Mt} regulon genes displayed intrinsic differential expression in the Δ Rv1625c strain relative to WT (Fig 8C) but were not universally differentially expressed in response to cAMP induction. This suggests that Rv1625c might play a native role in regulating some CRP_{MT} operon genes during cholesterol utilization. Overall, these findings are significant because they demonstrate that only a subset of CRP_{Mt} operon genes are altered either in response to induction of cAMP synthesis, or through loss of Rv1625c, in the presence of cholesterol. While this study does not explain the native role of CRP_{MT} during infection, V-59 and TetOn-cAMP can be used as tools in future studies to examine regulation of this operon under different growth conditions or during infection which may provide insight into its function in Mtb pathogenesis.

mCLB073 is an optimized analog of the V-59 compound series

Next, we sought to identify chemical features that are essential in a potent Rv1625c agonist, and to develop an optimized compound for use during *in vivo* studies. The screening hit (V-59) was relatively potent against Mtb in macrophages and had several satisfactory pharmacological features including plasma exposure above the EC₅₀ (as determined in cholesterol media) for approximately 24 hours following oral dosing in mice at 20 mg/kg (Fig 2). We sought to improve the properties of the V-59 compound series with medicinal chemistry. Structure activity relationship studies determined that replacing the tetrazole ring in V-59 with the oxadiazole ring in mCIS635 improved potency and slightly improved solubility. Replacing the 4-methyl-1,2,5-oxadiazole ring in V-59 with a 1-methyl-1H-1,2,4-triazole ring addressed the liability of the oxadiazole ring and generated the lead compounds mCLE299, mCLF177, mCLF178, and mCLB073 that had improved properties including better potency and extended plasma exposure following oral administration in mice. We explored constraining the piperidine ring in order to increase compound solubility by lowering its lattice energy, through an azabicyclic ring and a chiral center in several molecules of this series (Fig 2 and S2 Table). Interestingly, the *cis* isomer (mCLF024) displayed potency similar to the advanced lead compounds in this series, while the *trans* isomer (mCLF025) was inactive (S2 Table).

Among the optimized analogs, the lead compound (1-(4-(3-(3,4-dichlorophenyl)-1,2,4-oxadiazol-5-yl)-1-piperidinyl)-2-(2-methyl-2H-1,2,4-triazol-3-yl)-1-ethanone), named mCLB073, exhibited a ~17-fold potency improvement against Mtb in cholesterol media relative to V-59 while maintaining excellent pharmacokinetic properties and a good safety profile. We then verified that mCLB073 retained on-target activity. The Δ Rv1625c strain was refractory to mCLB073 treatment (S2B Fig), and mCLB073 activates cAMP synthesis (Figs 3B and S2C). Additionally, we isolated spontaneous resistant mutants in Mtb cultured with mCLB073. All spontaneous resistant mutants we isolated contained mutations in *rv1625c* that conferred resistance to mCLB073 and cross-resistance to V-59 (Figs 3C and S2A). These results indicate that mCLB073 is a genuine Rv1625c agonist. When dosed orally in mice, mCLB073 maintained plasma exposure over the EC₅₀ identified in cholesterol media for at least 24 hours (Fig 2). This demonstrated that mCLB073 is suitable for once-daily oral dosing in mouse models of infection and justified using this compound as a chemical probe during *in vivo* studies.

Selective activation of cAMP synthesis inhibits Mtb pathogenesis in vivo

Next, we examined whether treatment with Rv1625c agonists would alter Mtb survival in a mouse model of infection. We infected BALB/c mice with WT Mtb via the intranasal route, and administered a vehicle control, V-59, or isoniazid by oral gavage once-daily during weeks 4 through 8 post-infection. V-59 (50 mg/kg) caused a ~ 0.4 -log₁₀ reduction in lung CFUs and reduced the extent of lung inflammation by $\sim 50\%$ (Fig 9A and 9B). Similar results were obtained in CFU counts (~ 0.5 -log₁₀ reduction) in the lungs of C3HeB/FeJ mice infected and treated in the same manner (Fig 9C and 9D). The C3HeB/FeJ Mtb infection model was used

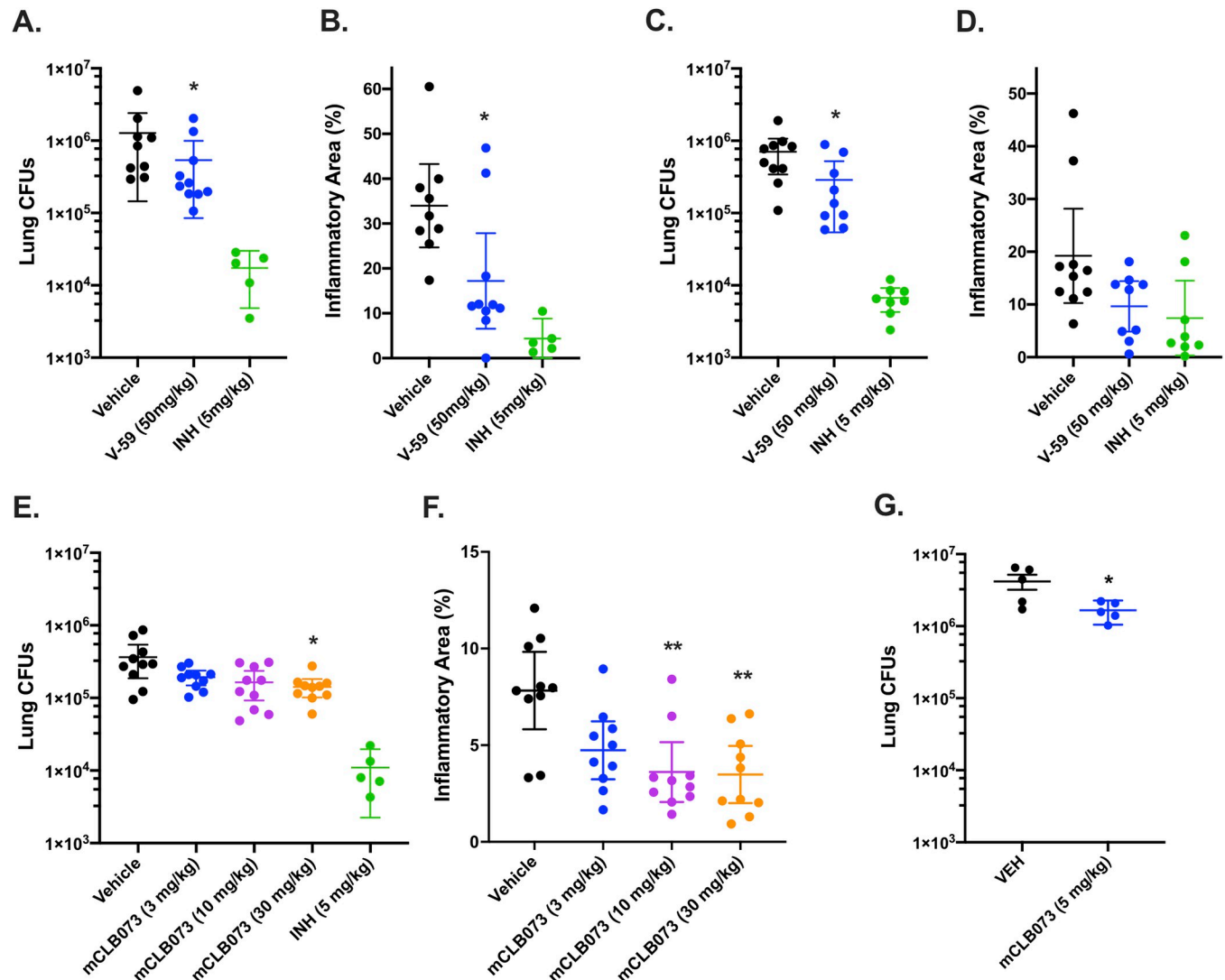


Fig 9. Chemically activating Rv1625c reduces Mtb pathogenesis *in vivo*. Effect of V-59 treatment on bacterial burden and pathology in the lungs of BALB/c (A and B) or C3HeB/FeJ mice (C and D). In (A–D) mice were infected and treated with V-59, INH, or vehicle control. Data are from two independent experiments with 5 mice (A and B), or one experiment with 10 mice (C and D) per group. Outliers with CFUs below the infectious dose were excluded from the analyses (* $P < 0.05$, Mann-Whitney test). (E and F) Impact of mCLB073 treatment on bacterial burden (E) and pathology (F) in BALB/c mice infected and treated with the indicated doses of mCLB073, INH, or vehicle control (* $P < 0.05$, ** $P < 0.01$, Kruskal-Wallis test and Dunn's multiple comparisons test). Infections in (A–F) were by the intranasal route. Data are from one experiment with 10 mice per group. (G) Impact of mCLB073 treatment on bacterial burden in BALB/c mice infected by aerosol and treated with 5mg/kg mCLB073 or vehicle control. Data are from one experiment with 5 mice per group (* $P < 0.05$, Kruskal-Wallis test and Dunn's multiple comparisons test). All data are shown as means \pm SEM.

<https://doi.org/10.1371/journal.ppat.1009862.g009>

because these mice produce type I IFN- and neutrophil-driven pathology that results in well-organized necrotic granulomas containing high numbers of extracellular bacterial [46–49]. Thus, the finding that an Rv1625c agonist inhibits bacterial growth and limits lung pathology in both a relatively resistant and a susceptible model of TB suggests that this compound series could be effective despite the heterogeneous host response mounted in Mtb infections [50]. To verify the improved potency of mCLB073 against Mtb *in vivo*, we infected BALB/c mice with WT Mtb via the intranasal route, and administered a vehicle control, mCLB073, or isoniazid by oral gavage once-daily during weeks 4 through 8 post-infection. Treatment with mCLB073 (30mg/kg) reduced Mtb CFUs in the lungs of mice significantly (~ 0.4 -log₁₀ reduction) (Fig 9E) and decreased the extent of lung pathology by $\sim 45\%$ (Fig 9F). In a separate study of BALB/c mice that were aerosol infected and treated in the same manner, we observed a significant reduction in lung CFUs (~ 0.4 -log₁₀ reduction) at a lower dose of mCLB073 (5mg/kg) which further confirms the improved pharmacological properties of mCLB073 (Fig 9G).

Because the mechanism of action of mCLB073 is novel, we tested whether mCLB073 treatment would lead to increased tolerance to a frontline TB drug (rifampicin) during infection. We found that the addition of mCLB073 (30 mg/kg) to a sub-optimal dose of rifampicin did not increase the bacterial burden in the lungs of BALB/c mice, suggesting this mechanism of action does not promote tolerance to other TB antibiotics (S5E Fig). Finally, we addressed the potential concern that this chemotype would activate off-target, mammalian AC enzymes. We found no evidence that V-59 activates ACs in mammalian cells (S5F Fig), and the low toxicity profile of the Rv1625c-activating compounds (Fig 2) suggests limited off-target activation of mammalian ACs. These results demonstrate the increased potency of mCLB073 relative to V-59 *in vivo*, and suggest that chemically activating cAMP synthesis in Mtb during chronic infection confers a fitness cost to the bacterium.

Discussion

Mtb possesses an expanded repertoire of cAMP signaling pathway components compared to other bacteria, suggesting this is an important mechanism to coordinate physiological functions in response to environmental cues. However, how Mtb physiology can be regulated through cAMP signaling, particularly through activation of specific AC enzymes, is not well understood. It was also not previously established whether this signaling pathway could be manipulated pharmacologically to disrupt Mtb pathogenesis. This gap in knowledge is partly explained by the lack of chemical and genetic tools that are equivalent to the eukaryotic AC agonist forskolin in the Mtb system. In this study we identified a chemical AC agonist that is suitable for *in vitro* and *in vivo* studies. And in a complementary approach, we created and validated a TetOn-cAMP construct that permits dose-dependent induction of cAMP synthesis in Mtb. These tools allowed us to establish a link between induction of cAMP synthesis, downregulation of cholesterol utilization, and inhibition of Mtb pathogenesis during infection.

Here, we re-examined a collection of compounds that were identified in a high-throughput screen as inhibitors of Mtb growth in macrophages and cholesterol media. Based on a previous study [29] we knew that this collection contained at least three Rv1625c-dependent compounds, and sought to identify an additional Rv1625c agonist with improved potency and acceptable properties for use in *in vivo* studies. From the screening hits, we identified a candidate small molecule named V-59 that displayed promising pharmacological properties (Fig 2). We then determined that growth inhibition by V-59 in cholesterol media and in macrophages requires a functional Rv1625c enzyme (Figs 1A, 1C and 3C), and V-59 induces cAMP synthesis in an Rv1625c-dependent manner (Fig 3A and 3B). By quantifying degradation of the A-ring of cholesterol, we found that V-59 indeed blocks cholesterol utilization, in a mechanism

that requires the cyclase domain of Rv1625c (Fig 4). Our combined results strongly suggest that V-59 binds to the Rv1625c enzyme to activate AC activity, which artificially increases cAMP synthesis in Mtb to inhibit cholesterol utilization and impairs bacterial growth in cholesterol media and macrophages. However, we have not yet established a direct interaction between V-59 and Rv1625c using recombinant protein assays. This will be essential in the future to confirm that Rv1625c is activated by V-59 directly rather than through an unknown, indirect intermediate.

To study the impact of cAMP induction independent of V-59 and Rv1625c, we developed a TetOn-cAMP construct that increases cAMP synthesis in a dose-dependent manner (Fig 5A). We found that inducing cAMP synthesis is sufficient to decrease growth of Mtb in cholesterol media (Fig 5B) and to block cholesterol degradation (Fig 5C). Transcriptional studies revealed hallmarks indicating that cholesterol degradation is inhibited early in the breakdown process following V-59 treatment, or induction of cAMP synthesis via the TetOn-cAMP construct (Figs 6 and 7). Together, this demonstrates that inducing cAMP through a different AC is sufficient to mimic the effects of an Rv1625c agonist, which suggests that AC activation is a general mechanism that can be leveraged to inhibit cholesterol utilization in Mtb. However, the experiments presented here did not address how native activation of the many individual ACs present in Mtb may work together to differentially regulate distinct physiological pathways, and this is a question that warrants future investigation. Collectively, our findings indicate that chemically or genetically inducing cAMP synthesis in Mtb above a certain threshold inhibits cholesterol degradation, blocks transcriptional activation of hallmark cholesterol utilization genes, and decreases propionyl-CoA pools in proportion to the amount of cAMP induced. Cholesterol breakdown is a many-stage process, and side chain and ring degradation can occur in tandem [6]. Considering this, one interpretation consistent across these results is that robust activation of cAMP synthesis prevents cholesterol side chain and ring degradation simultaneously, and this decreases the breakdown of cholesterol to an early intermediate that is required to de-repress the KstR1 regulon.

While investigating the effect of V-59 on Rv1625c activity and cholesterol utilization, we unexpectedly discovered that the six-helical transmembrane domain of Rv1625c and the associated N-terminal cytoplasmic tail is intrinsically required for complete cholesterol degradation in Mtb (Fig 4A and 4B). Given that Rv1625c had no previously predicted role in cholesterol utilization, this is a surprising connection between the AC that V-59 activates, and the metabolic pathway it inhibits. The native function of Rv1625c signaling during infection is not established, and Rv1625c is the only AC that has been linked to a specific downstream metabolic pathway in Mtb thus far [23]. Our finding that the Rv1625c transmembrane domain is required for cholesterol ring catabolism expands on work by others showing that the catalytic domain is not the only functionally relevant component of this AC [32,33,51], but the mechanism that mediates its involvement in cholesterol catabolism remains to be determined. It is not known if the transmembrane domain of Rv1625c mediates protein-protein interactions that are required to complete cholesterol catabolism and whether this, or an alternative mechanism, is involved in maximizing regulation of cholesterol utilization by Rv1625c agonists. It is notable that the cholesterol utilization defect in the Δ Rv1625 strain was likely limited to ring catabolism (Fig 4A), and was not sufficient to impact bacterial growth in cholesterol media or macrophages (Fig 1A and 1C), or to inhibit transcriptional activation of methylcitrate cycle genes by liberation of propionyl-CoA (Figs 6 and 7A). Because degradation of the cholesterol side chain and rings can proceed in tandem, it is conceivable that a blockage in ring catabolism could be present in Δ Rv1625 Mtb, while growth on cholesterol and liberation of propionyl-CoA and acetyl-CoA from the side chain are maintained. Two genes neighboring Rv1625c (*rv1626/pdtA* and *rv1627c*) have been predicted to be required during cholesterol utilization

[45]. It will be helpful to determine whether Rv1625c interacts with these proteins, or others capable of regulating lipid metabolism in Mtb. Moreover, it would be interesting to examine whether the binding of V-59 to Rv1625c not only activates cAMP synthesis but also alters an interaction between Rv1625c and a relevant protein. This would help explain the distinct but overlapping cholesterol utilization defects we observed in WT Mtb treated with V-59, the Δ Rv1625 strain, and TetOn-cAMP Mtb treated with different doses of Atc. The amount of cAMP produced by the TetOn-cAMP strain was most similar to V-59 treatment at the lower dose of Atc (50 ng/mL) tested (Fig 5A). This dose was also correlated with less severe defects in growth in cholesterol media, $^{14}\text{CO}_2$ release from [4- ^{14}C]-cholesterol, and propionyl-CoA liberation from cholesterol than the defects observed with V-59 treatment (Figs 5B, 5C and 7B). Based on this and our observations in the Δ Rv1625 strain, it is interesting to speculate that V-59 interacts with the Rv1625c protein, altering both a relevant protein interaction and increasing cAMP synthesis, both of which contribute to V-59's total effect on cholesterol utilization. However, the mechanism and kinetics of inducing cAMP synthesis with the TetOn-cAMP system are distinct from V-59 treatment, limiting our ability to conclude that a particular dose of Atc mimics V-59 treatment. Future experiments to identify cholesterol degradation intermediates that accumulate in WT Mtb treated with V-59 could help clarify this by allowing comparison of step(s) of the cholesterol degradation pathway that are blocked by V-59 treatment versus TetOn-cAMP induction or loss of the Rv1625c protein alone.

These findings expand our limited understanding of how cAMP signaling can alter metabolism in Mtb, and it remains to be determined whether a downstream cAMP-binding protein is required for V-59 or TetOn-cAMP induction to inhibit cholesterol utilization in Mtb. We investigated Rv0998/Mt-Pat because it is a cAMP-binding lysine acetyltransferase that was previously shown to acetylate and inactivate the acetyl-CoA/propionyl-CoA ligase (Rv3667/Acs) and various FadD enzymes in Mtb, which can regulate incorporation of 2- and 3-carbon precursors into central metabolism [27,28]. Mt-Pat was not required for V-59 to inhibit Mtb growth (S5A Fig) or induction of MCC genes (S5B Fig) in cholesterol media. This is consistent with data showing that acetate rescues growth during both V-59 treatment and TetOn-cAMP activation (Figs 1B and S5C), suggesting Acs has not been inactivated by Mt-Pat in either condition. The FadD enzyme Rv3515c/FadD19 initiates cholesterol side chain degradation [6] but FadD19 is not a confirmed target of inactivation by Mt-Pat, and other FadD enzymes that are known to be acetylated by Mt-Pat are not established steps in cholesterol breakdown [28].

Although Mt-Pat likely does not mediate inhibition of cholesterol utilization downstream of V-59 treatment or TetOn-cAMP induction, it is unclear whether any of the other eleven predicted cAMP-binding proteins in Mtb are involved in this mechanism [23]. We examined the predicted operon of one other cAMP-binding protein, the transcription factor CRP_{MT}, and found that only a handful of these genes were differentially expressed in a cAMP-dependent and/or Rv1625c-dependent manner during growth in cholesterol media (Fig 8). Notably, three of these genes are required for optimal growth of Mtb in cholesterol media and/or in mouse models of TB, but are not directly involved in cholesterol side chain or ring breakdown [12,45]. Most of the remaining genes do not have established functions, making it difficult to predict how changes in their expression could impact specific aspects of Mtb physiology. Further experiments are needed to determine whether these transcriptional changes are indeed mediated through CRP_{MT} activity, and whether this contributes significantly to the cholesterol utilization defects observed in Mtb during V-59 treatment or in the Δ Rv1625c strain. Alternatively, because cholesterol uptake by the bacterium and initiation of cholesterol side chain breakdown by FadD19 are both ATP-dependent processes, it is possible that ATP depletion occurring during increased cAMP synthesis mediates inhibition of cholesterol utilization. Considering the large number of cAMP signaling pathway components present in Mtb, the

mechanisms by which distinct ACs and downstream cAMP-responsive proteins can coordinate different physiological responses under native inducing conditions requires further investigation.

Compared to the previously-published Rv1625c agonist V-58 [36], V-59 represents a significant advance because it is an Rv1625c agonist that is suitable for use in an *in vivo* model of TB. V-59 also provided a basis for understanding how to improve Rv1625c agonists through medicinal chemistry. We completed a medicinal chemistry effort focused on addressing the structural liabilities of V-59 and improving the potency of its activity against Mtb. This identified mCLB073, a stable molecule with improved potency and desirable chemical, pharmacological, pharmacokinetics and safety properties, which makes it a good drug candidate for clinical testing and a useful compound for further *in vivo* studies of this pathway in Mtb. While investigating the potency of compounds in this series with constrained piperidine rings, we also identified molecules whose potency differed widely based on the chirality of their azabicyclic rings. In the future, it would be interesting to identify the underlying explanation for the differential potency of these compounds on Rv1625c activity through structural biology.

Chemical tools like V-59/mCLB073 that can be used to modulate distinct pathways in Mtb in infection models are valuable because it is difficult to predict the *in vivo* metabolic state and vulnerabilities Mtb experiences during infection [52–56]. We developed V-59/mCLB073 as compounds that can effectively modulate cAMP synthesis and block cholesterol utilization in Mtb, while being suitable for *in vivo* studies. Single-agent studies using V-59/mCLB073 established that cAMP induction modestly impairs bacterial growth and lung pathology in mouse models of TB (Fig 9). A recent study also found that the “MKR superspreader” strain of Mtb, an emergent multidrug-resistant strain of the modern Beijing lineage, displayed enhanced upregulation of cholesterol utilization genes during macrophage infection relative to the H37Rv reference strain [13]. V-59 was used to show that activating Rv1625c to inhibit cholesterol utilization in the MKR strain selectively reduced intracellular survival of the bacteria in infected macrophages [13]. This suggests that efficacy of Rv1625c agonists may be potentiated by cholesterol-related metabolic adaptations that are especially crucial to the intracellular survival of at least one multi-drug resistant strain of Mtb. Identifying this link between cAMP signaling, cholesterol utilization, and Mtb fitness during infection is important because it is challenging to target metabolic pathways in Mtb that are not redundant and are sufficiently distinct from human pathways to limit side-effects [27,52,57]. Numerous studies have suggested that cholesterol utilization is a key metabolic adaptation that supports Mtb survival during chronic infection [7–11], but the efficacy of single-step inhibitors of cholesterol degradation may be limited, unless they are able to cause accumulation of toxic metabolites in the bacterium [6,8–10,58]. Inhibitors that block this pathway early and/or shut down multiple steps present one desirable alternative. This study revealed that the Rv1625c agonists V-59/mCLB073 are an improvement over the single-step cholesterol degradation inhibitors we reported previously; these compounds inhibit cholesterol catabolism early and/or at both side chain and ring degradation steps and display excellent pharmacokinetic properties. The optimized compound mCLB073 will facilitate future studies examining how Rv1625c agonists alter Mtb fitness in animal models that more faithfully recapitulate the complexities of the granuloma microenvironment present in human TB. Much remains to be discovered about the restrictions Mtb encounters *in vivo* when the bacterium can co-catabolize multiple complex substrates. Future infection studies that combine V-59/mCLB073 treatment with chemical or genetic modulation of other pathways in Mtb may provide interesting insights on this topic and reveal how to optimize disruption of Mtb fitness during V-59/mCLB073 treatment.

In summary, we have shown here that activating cAMP synthesis in Mtb, either by activating Rv1625c AC activity with a small molecule agonist or by inducing expression of the

minimal catalytic subunit of Rv1264, blocks cholesterol degradation. Rv1625c is also the first AC in Mtb to be linked directly to a particular downstream pathway. Mtb has a cadre of structurally-diverse ACs and predicted cAMP-binding proteins with mostly uncharacterized functions, which may represent potential to alter pathways beyond cholesterol utilization in this bacterium. However, it is unknown whether agonists for ACs other than Rv1625c would have comparable downstream effects in Mtb. In other pathogenic bacteria, cAMP signaling is known not only for coordinating changes to carbon metabolism, but also for mediating diverse functions including biofilm formation, virulence gene expression, and secretion systems [14]. This study identified AC agonists suitable for *in vivo* studies of cAMP signaling in Mtb, which revealed that chemically activating cAMP synthesis may be an untapped mechanism for manipulating bacterial fitness during infection, redefining the traditional mechanism for an anti-virulence compound. In Mtb, AC activation is able to stall at least one metabolic pathway that supports *in vivo* survival, with the potential to yield a new antibiotic. It is interesting to speculate whether additional AC agonists could be developed as tools to study cAMP signaling during infection, or as antibiotics, in other bacteria. The mechanism(s) by which inducing cAMP synthesis modulates cholesterol utilization in Mtb is not yet fully explained, and will be an important area for future studies as our knowledge of the role cAMP signaling plays in Mtb physiology continues to expand.

Materials and methods

Ethics statement

Animal work was approved by Cornell University IACUC (protocol number 2013–0030). All protocols conform to the USDA Animal Welfare Act, institutional policies on the care and humane treatment of animals, and other applicable laws and regulations. Isoflurane was delivered via nebulizer for anesthesia during oral delivery of compounds. Euthanasia was performed via delivery of carbon dioxide.

Bacterial culture

Unless noted, Mtb strains were grown in Middlebrook 7H9 medium supplemented with glycerol and OADC (oleic acid, albumin, dextrose, catalase) (Difco). 7H12 medium contained Middlebrook 7H9 powder (Becton Dickinson), 0.1% casitone, and 100 mmol MES free acid monohydrate, pH 6.6. Prior to culturing in media containing different carbon sources, bacteria were washed in 7H12 media without additional carbon sources. Cholesterol was added as tyloxapol:ethanol micelles to a final concentration of 100 μ M [29]. Where specified, 0.1% acetate was added. All liquid media contained 0.05% tyloxapol (Acros Organics). Mtb was cultured on Middlebrook 7H10 agar supplemented with glycerol and OADC (Difco). Strains were maintained with selective antibiotics as described in (S3 Table). Anhydrotetracycline was prepared in 100% EtOH and used at final concentrations of 500 ng/mL or 50 ng/mL. Cytotoxicity and ADME assays are described in (S1 File), chemical synthesis is described in (S2 File), and NMR analysis of synthesized compounds is described in (S4 File).

Construction of mutants and TetOn-cAMP strains

The *rv1625c* gene was disrupted in CDC1551 Mtb using allelic exchange [38]. Δ Rv1625c was complemented by overexpressing full-length Rv1625c or the transmembrane domain (amino acids V1-D204), from an integrating vector under the control of the *hsp60* promoter. The TetOn-cAMP strain expresses the His-tagged catalytic domain of Rv1264, under control of the *p606* Atc-inducible promoter. A single amino acid change (D265A) was introduced in the

rv1264 sequence using site-directed mutagenesis. Base pairs 794–795 were mutated (GAC to GCG) and confirmed by sequencing. Details of strains and constructs are listed in (S3 Table).

Growth inhibition measurements

Growth assays were conducted by inoculating Mtb strains into liquid media at an OD₆₀₀ of 0.05, and measuring the OD₆₀₀ at three-day intervals. Compounds were added at the indicated concentrations initially and every three days throughout. For EC₅₀ measurements, Mtb strains were pre-grown in 7H12+acetate media and assayed as described [29]. For macrophage infections, bone marrow-derived macrophages (BMDMs) were isolated and differentiated from BALB/c mice [38]. BMDMs were seeded in media without antibiotics in 24-well plates before infection. Cells were infected with Mtb. After 2 hours, extracellular bacteria were removed and replaced with fresh media containing indicated treatments. Media was replaced every 24 hours for the duration of the experiment. Fold changes in CFU's were determined by lysing macrophages in SDS (0.01%) and plating on agar plates.

¹⁴CO₂ release experiments

Catabolism of [4-¹⁴C]-cholesterol to ¹⁴CO₂ was quantified as described previously, with minor modifications [38]. Briefly, Mtb cultures were pre-grown in 7H12+cholesterol+acetate media for one week and adjusted to an OD₆₀₀ of 0.5. DMSO or V-59 were added 45 minutes prior to adding [4-¹⁴C]-cholesterol. For TetOn-cAMP experiments, bacteria were inoculated at an OD₆₀₀ of 0.1 into 7H12+cholesterol+acetate media and treated with EtOH, Atc, or V-59 at the indicated concentrations overnight, and again one hour prior to beginning the ¹⁴CO₂ release assay. Cultures were adjusted to an OD₆₀₀ of 0.5 in their respective media and [4-¹⁴C]-cholesterol was added. In both cases, ¹⁴CO₂ released from the vented Mtb culture flasks was collected as described [38].

Thin-layer chromatography

Mtb cultures were grown to an OD of 0.6, then inoculated at an OD₆₀₀ of 0.4 into 7H12+cholesterol media for three days. Cultures were concentrated in their respective media, then [4-¹⁴C]-cholesterol was added, the culture supernatant was collected after 24 hours, extracted in ethyl acetate, quantified by scintillation counting, and equal counts (10,000 CPM per lane) were spotted for each sample on a silica gel TLC plate (EMD Chemicals). Plates were developed in toluene:acetone (75:25, v/v) and imaged by phosphorimaging.

Heterologous expression of Rv1625c in *cya*⁻ *E. coli*

The *cya*-deficient *E. coli* strain HS26, derived from the TP610 strain, was transformed with the pMBC530 plasmid expressing the full Rv1625c ORF or the empty vector control plasmid pMBC529 and the strains were grown and induced as previously described [36]. After 18 hours, sample OD₆₀₀ values were recorded and supernatants were collected and used to quantify cAMP by ELISA.

Quantification of bacterial cAMP

Bacteria were pre-grown in 7H12+cholesterol+acetate before inoculation into fresh media at an OD₆₀₀ of 0.1 containing either a cAMP-inducing compound (V-59 or Atc) or vehicle control. After 24-hour incubation, bacteria were collected by centrifugation, and the supernatant was reserved to measure secreted cAMP. The pellet was washed with fresh media, resuspended in lysis buffer (0.1M HCl, 1% Triton X-100 in H₂O), and disrupted by bead beating (MP

Biomedical). Cell-free lysates were reserved to measure internal cAMP by ELISA (Enzo Life Sciences). The sum of the internal and external values, or the external values alone, for each sample were used to estimate the total cAMP produced per 1×10^8 bacteria.

RNA-seq analysis

Bacteria were cultured in 7H9OADC before inoculation into fresh media containing a cAMP-inducing compound (10 μ M V-59 or 500 ng/mL Atc) or vehicle control (DMSO or EtOH) at an OD₆₀₀ of 0.1. The following day, bacteria were inoculated into 7H12+cholesterol media containing fresh compound or vehicle control. After four hours, cultures were pelleted by centrifugation, washed with guanidine thiocyanate-based buffer and stored at -80°C. Pellets were washed and suspended in Trizol LS (Ambion) and lysed by bead beating. Total RNA was isolated by chloroform extraction and precipitated in isopropanol with GlycoBlue reagent (Thermo Fisher). RNA was resuspended in nuclease-free water, genomic DNA contamination was removed using the Turbo-DNA free kit (Invitrogen), and rRNA was depleted using the Ribo-Zero Gold rRNA removal kit (Illumina). Sample quality was determined via Fragment Analyzer (Advanced Analytical) and TruSeq-barcoded RNAseq libraries were generated with the NEBNext Ultra II Directional RNA Library Prep Kit (New England Biolabs). Sequencing was performed at the Cornell University Transcriptional Regulation and Expression Facility on a NextSeq500 instrument (Illumina) at a depth of 15 M single-end 75 bp reads. Reads were trimmed for low quality and adaptor sequences with TrimGalore, and aligned to the *Mycobacterium tuberculosis* CDC1551 reference genome (GCA_000008585.1) with STAR. DESeq2 was used with default parameters and alpha = 0.05 to generate the differential gene expression results (S3 File). Multiple test correction was performed using the Benjamini Hochberg method.

Propionyl-CoA reporter assays

Fluorescent *prpD*::GFP assays in liquid media were conducted in 7H12+cholesterol+acetate as described [38]. BMDMs were infected at an MOI of 5. Extracellular Mtb was removed after 2 hours, and replaced with fresh media containing DMSO or V-59. For intracellular TetOn-cAMP experiments, the TetOn-cAMP *prpD*::GFP strain was pre-induced in 7H9OADC media with EtOH, Atc (500 ng/mL), or V-59 (10 μ M) for 24 hours prior to infection. After extracellular Mtb was removed, fresh media containing EtOH, Atc (3 μ g/mL), or V-59 (10 μ M) was added to the infected BMDMs. After 24 hours, infected BMDMs were scraped and fixed in paraformaldehyde. Fixed BMDMs were suspended in lysis buffer (0.1% SDS, 0.1 mg/mL Proteinase K in H₂O) and lysed by passage through a 25-gauge needle. Pellets were retained for analysis. The GFP MFI was quantified from 10,000 bacteria by flow cytometry and analyzed using FlowJo (Becton Dickinson). Details of reporter plasmid constructs are listed in S3 Table.

Pharmacokinetic studies

Pharmacokinetic profiles were determined in male CD-1 mice after single dose oral administration (20 mg/kg). Stock solutions were prepared in 75% PEG 300, 25% D5W. An aliquot of the dose solutions was taken before and after dosing, and stored at -20°C for subsequent analysis. Blood samples were collected at standard time points through a retro-orbital bleed from 3 mice per time point. Heparinized blood was collected from each mouse and centrifuged to separate plasma for quantification of drug concentration by LC/MS analysis.

Analysis of spontaneous resistance to mCLB073

The frequency of spontaneous resistance to mCLB073 *in vitro* was estimated by plating Mtb on cholesterol agar plates containing mCLB073 (25 μ M to 100 μ M). Cholesterol was dissolved in 500 mM methyl- β -cyclodextrin and added to 7H10 agar at 100 μ M. 7×10^5 CFU WT Erdman Mtb was spread per 150 mm plate and colonies were enumerated. Mutant clones were isolated, and subjected to EC₅₀ assay. The *rv1625c* region was amplified by PCR and sequenced to determine the location of each mutation.

Mouse infections

Six to eight-week-old BALB/cJ mice (Jackson Laboratories) were infected with 1000 CFU of Erdman Mtb intranasally. C3HeB/FeJ (Kramnik) mice (Jackson Laboratories) were infected with 500 CFU of Erdman Mtb intranasally. At weeks 4 through 8 post-infection, compounds or vehicle controls were administered once-daily by oral gavage. For aerosol infection, BALB/cJ mice (Jackson Laboratories) were infected via an aerosol inhalation exposure system (Glass-Col) with a calibrated dose of 200 CFU of Erdman Mtb. Experimental compounds or vehicle control were administered once-daily at weeks 4 through 8 post-infection by oral gavage. After treatment, lung tissues were collected and processed for histology and CFU enumeration. For CFUs, lungs were homogenized in PBS, 0.05% Tween-80 and plated on 7H10 OADC. Inflammatory area was scored by measuring the percent of tissue inflamed (granulomatous tissue with peripheral and peribronchial lymphocytes and plasma cells) per low power microscopic field. In a blinded fashion, 4–15 fields were analyzed per lung sample.

Statistical analysis

Averages were chosen as a measure of central tendency throughout. Analyses were performed using GraphPad Prism. When data were expected to fit an approximately normal distribution One-way ANOVA was applied. For multiple comparisons between pre-selected pairs of control versus treatment groups, Sidak's multiple comparisons test was used. For comparisons between multiple treatment groups relative to a single control group, Dunnet's multiple comparisons test was selected. Two-way ANOVA with Tukey's multiple comparisons test was used when it was necessary to analyze the impact of both the strain background and compound versus control treatments. Data from mouse experiments were analyzed using non-parametric tests. For a single pre-planned comparison, a Mann-Whitney test was selected. For multiple comparisons, the Kruskal-Wallis test and Dunn's multiple comparisons test were used. Differences with *P* values < 0.05 were considered significant. For RNA-seq results, significance of the log₂ fold-change between groups was assigned based on the adjusted *p*-value for differential expression analysis, where significance was assigned when the *P*-adj value was < 0.05.

Supporting information

S1 Fig. The inhibitory activity of V-59 in cholesterol media is dependent on Rv1625c. (A) Inhibitory activity of V-59 against WT, the Rv1625c transposon mutant (Tn::*rv1625c*), and WT transformed with an overexpression plasmid expressing the *rv1625c* gene (2*xrv1625c*) in 7H12+cholesterol media. (B) Inhibitory activity of V-59 against WT, Δ Rv1625c, and Comp_{full} in 7H12+cholesterol media (left) or 7H12+cholesterol+acetate media (right). Data shown are representative, from one experiment with two technical replicates. Symbols are mean data points, and curves display nonlinear fit of dose-response. (C) Effect of V-59 on growth of Mtb in murine macrophages. Macrophages were infected at an MOI of 2 (left), 1 (middle), or 0.5 (right) and treated with V-59 (25 μ M) or DMSO. Data for MOI of 2 are from three

experiments, with two or three technical replicates each. Data for MOI of 1 and 0.5 are from one experiment with two or three technical replicates each. Data are shown as means \pm SD. Each symbol indicates one replicate. **(D)** Effect of frontline antibiotics on WT and Δ Rv1625 in 7H12+cholesterol (INH, RIF, EMB) or in MES-buffered 7H9OADC+glycerol, pH 5.9 (PZA). Data shown are representative, from one experiment with two technical replicates. Symbols are mean data points, and curves display nonlinear fit of dose-response. **(E)** RNA-seq derived normalized counts of *rv1625c* reads in WT, Δ Rv1625c, and Comp_{Full} strains in 7H12+cholesterol media.

(PDF)

S2 Fig. The activity of mCLB073 is dependent on Rv1625c. **(A)** Inhibitory activity of mCLB073 or V-59 against spontaneous resistant mutants that were generated during culture with mCLB073. **(B)** Inhibitory activity of mCLB073 against WT or Δ Rv1625c in 7H12+cholesterol media. Data shown are representative, from one experiment with two technical replicates. Symbols are mean data points, and curves display nonlinear fit of dose-response. **(C)** Impact of mCLB073 on cAMP production in WT Mtb. ELISA was used to quantify cAMP from lysed cells 24 hours after addition of mCLB073, or vehicle control (DMSO). Data is from one experiment, with two technical replicates. Data are shown as means \pm SD.

(PDF)

S3 Fig. An intact cyclase domain of Rv1625c is required for V-59 to inhibit cholesterol degradation. **(A)** Catabolic release of $^{14}\text{CO}_2$ from [U- ^{14}C]-palmitate in media containing fatty acid. EtOH (control), V-59, or Atc were added to the TetOn-cAMP Mtb cultures 24 hours prior to the start of the experiment. Data are from one experiment with three technical replicates, normalized to OD and quantified relative to EtOH control. Data are shown as means \pm SD **(B)** Catabolic release of $^{14}\text{CO}_2$ from [4- ^{14}C]-cholesterol in media containing cholesterol and acetate. V-59 (10 μM) was added to the cultures once at the beginning of the experiments and DMSO was used as a vehicle control. Data are from one experiment with three technical replicates, normalized to OD and quantified relative to WT treated with DMSO. Data are shown as means \pm SD. **(C)** Schematic illustrating the topology of the N-terminal transmembrane domain and essential residues of the C-terminal cyclase domain of Rv1625c (left). Schematics illustrating modified Rv1625c constructs used in these studies (center and right).

(PDF)

S4 Fig. Construction and validation of TetOn-cAMP constructs. **(A)** Schematic illustrating the domains of the native Rv1264 adenylyl cyclase (left) and the design of the TetOn-cAMP construct (right). The TetOn-cAMP construct contains the minimum-necessary cyclase domain of Rv1264, and lacks the pH-sensitive inhibitory domain of the native Rv1264 protein. Expression of the cyclase domain is under control of a TetOn promoter. Upon treatment with Atc, release of the tetracycline repressor (TetR) causes initiation of transcription of the Rv1264 catalytic domain. The C-terminal end of the cyclase domain is His-tagged to allow immunoblotting. **(B)** Immunoblots of bacterial lysates confirm that the TetOn constructs are expressed in the presence of Atc and not the vehicle control EtOH. The anti-His blot detects the Rv1264 cyclase domain and the anti-GroEL2 blot is the loading control. **(C)** Impact of inducing the TetOn-Rv1264_{D265A} construct in media containing cholesterol and acetate. Cultures were treated with one dose of EtOH, V-59 (10 μM), or Atc at the indicated concentrations and samples were collected 24 hours later for ELISA. Data are displayed as total cAMP per 10^8 Mtb. Data are from two independent experiments with two technical replicates each, shown as means \pm SD (** $P < 0.01$, One-way ANOVA with Dunnett's multiple comparisons test). **(D)**

Effect of inducing TetOn-Rv1264_{D265A} on the growth of Mtb in 7H12+cholesterol media, monitored by serial OD measurements. EtOH, V-59 (10 μ M), or Atc at the indicated concentrations were added initially and every three days for the duration of the experiment. Data are from one experiment with three technical replicates, shown as means \pm SD. (E) Catabolic release of ¹⁴CO₂ from [4-¹⁴C]-cholesterol in media containing cholesterol and acetate. The TetOn-Rv1264_{D265A} strain was treated with EtOH, V-59 (10 μ M), or Atc at the indicated concentrations overnight and again one hour prior to the beginning of the experiments. Data are from two independent experiments with three technical replicates each, normalized to OD and quantified relative to EtOH vehicle control. Shown as means \pm SD (not significant, Student's *t* test). (F) Relative GFP signal from the *prpD*::GFP reporter in response to inducing TetOn-Rv1264_{D265A} in media containing cholesterol and acetate. Cultures were treated with EtOH, V-59 (10 μ M), or Atc at the indicated concentrations. Data are normalized to EtOH vehicle control (***P* < 0.01, One-way ANOVA with Dunnett's multiple comparisons test). GFP MFI was quantified from 10,000 mCherry⁺ Mtb. Data are from two independent experiments with two technical replicates each, shown as means \pm SD. (PDF)

S5 Fig. Activating cAMP synthesis inhibits lipid metabolism in an Mt-Pat independent mechanism, and can inhibit fatty acid utilization without increasing antibiotic tolerance or increasing mammalian cAMP synthesis. (A) Inhibitory activity of V-59 against WT or Δ Mt-Pat in 7H12+cholesterol media. Data shown are from one experiment with two technical replicates. Symbols are mean data points, and curves display nonlinear fit of dose-response. (B) Relative GFP signal from the *prpD*::GFP reporter in WT versus Δ Mt-Pat strains carrying the TetOn-cAMP construct in media containing cholesterol and acetate. Cultures were treated in parallel with EtOH, V-59 (10 μ M), or Atc at the indicated concentrations. Data are normalized to EtOH vehicle control in each strain. GFP MFI was quantified from 10,000 mCherry⁺ Mtb. Data are from one experiment with two technical replicates, shown as means \pm SD. (C) Effect of inducing TetOn-cAMP on the growth of Mtb in 7H12+cholesterol+acetate media. EtOH, V-59 (10 μ M), or Atc at the indicated concentrations were added initially and every three days for the duration of the experiment. Data are from one experiment with three technical replicates, shown as means \pm SD. (D) Relative GFP signal from the *prpD*::GFP reporter in Mtb treated with V-59 or DMSO, in 7H12 media supplemented with C17:1 or propionate. Data shown normalized to WT+DMSO. GFP MFI was quantified from 10,000 mCherry positive Mtb. Data are from one experiment with two technical replicates, shown as means \pm SD. (E) Effect of mCLB073 treatment combined with a sub-optimal dose of rifampicin (RIF) in BALB/c mice infected by the aerosol route. Data are from one experiment with 10 mice per group (***P* < 0.01, Mann-Whitney test). Data are shown as means \pm SEM. (F) Quantification of cAMP in human cell lines treated with V-59 (10 μ M) or DMSO control. Data are from one experiment with two technical replicates, and are shown as means \pm SD. (PDF)

S1 Table. V-59 is structurally distinct from other cholesterol utilization inhibitors. Chemical structure of previously published single-step cholesterol breakdown inhibitors, and resynthesized analogs of previously described Rv1625c-dependent inhibitors. MW, molecular weight; --, not determined; EC₅₀, half-maximal effective concentration; hERG, human ether-à-go-go-related gene; CC₅₀, 50% cytotoxic concentration; PPB, plasma protein binding; IC₅₀, half-maximal inhibitory concentration; Cyp, cytochrome P450; ER, extraction ratio; PSA, polar surface area. (PDF)

S2 Table. Structures and activities of isomer compounds. MW, molecular weight; --, not determined; EC₅₀, half-maximal effective concentration; IC₅₀, half-maximal inhibitory concentration; ADME, absorption, distribution, metabolism, excretion; PPB, plasma protein binding; ER, extraction ratio; PO, per os.
(PDF)

S3 Table. Mtb strains used in these experiments.
(PDF)

S1 File. Supplementary materials and methods.
(PDF)

S2 File. Supplementary materials for chemical synthesis and analysis.
(PDF)

S3 File. RNA-seq dataset.
(XLSX)

S4 File. NMR analysis of synthesized compounds.
(PDF)

Acknowledgments

We thank Kathleen McDonough for pMBC529, pMBC530, and the HS26 *E. coli*. We thank Dirk Schnappinger for the TetOn plasmids. We thank Véronique Dartois and Jansy Sarathy for completing the caseum binding assays. We thank Jen Grenier, Ann Tate, and Faraz Ahmed from Cornell TReX for assisting with RNA-seq sample analysis.

Author Contributions

Conceptualization: Kaley M. Wilburn, H. Michael Petrassi, Brian C. VanderVen.

Formal analysis: Kaley M. Wilburn, Christine R. Montague, Bo Qin, Ashley K. Woods, Melissa S. Love, Case W. McNamara, Peter G. Schultz, Teresa L. Southard, H. Michael Petrassi, Brian C. VanderVen.

Funding acquisition: H. Michael Petrassi, Brian C. VanderVen.

Investigation: Kaley M. Wilburn, Christine R. Montague, Bo Qin, Ashley K. Woods, Melissa S. Love, Case W. McNamara, Teresa L. Southard, Lu Huang, Brian C. VanderVen.

Methodology: Kaley M. Wilburn, Christine R. Montague.

Resources: Brian C. VanderVen.

Supervision: Peter G. Schultz, H. Michael Petrassi, Brian C. VanderVen.

Visualization: Kaley M. Wilburn, Christine R. Montague.

Writing – original draft: Kaley M. Wilburn, H. Michael Petrassi, Brian C. VanderVen.

Writing – review & editing: Kaley M. Wilburn, Christine R. Montague, Bo Qin, Ashley K. Woods, Melissa S. Love, Case W. McNamara, Lu Huang, H. Michael Petrassi, Brian C. VanderVen.

References

1. World Health Organization. Global Tuberculosis Report 2019. (World Health Organization, Geneva, 2019).

2. Sarathy P.J, Dartois V. Caseum: a Niche for Mycobacterium tuberculosis Drug-Tolerant Persisters. *Clinical microbiology reviews* 33, (2020). <https://doi.org/10.1128/CMR.00159-19> PMID: 32238365
3. Hunter L. R., Jagannath C., Actor K, J. Pathology of postprimary tuberculosis in humans and mice: contradiction of long-held beliefs. *Tuberculosis* 87, 267–278 (2007). <https://doi.org/10.1016/j.tube.2006.11.003> PMID: 17369095
4. Peyron P., Vaubourgeix J., Poquet Y., Levillain F., Botanch C., Bardou F. et al. Foamy macrophages from tuberculous patients' granulomas constitute a nutrient-rich reservoir for M. tuberculosis persistence. *PLoS pathogens* 4, e1000204 (2008). <https://doi.org/10.1371/journal.ppat.1000204> PMID: 19002241
5. Kim J, M., Wainwright C, H., Locketz M., Bekker G, L., Walther B, G., Dittrich C. et al. Caseation of human tuberculosis granulomas correlates with elevated host lipid metabolism. *EMBO Molecular Medicine* 2, 258–274 (2010). <https://doi.org/10.1002/emmm.201000079> PMID: 20597103
6. Wilburn M, K., Fieweger A, R., VanderVen C, B. Cholesterol and fatty acids grease the wheels of Mycobacterium tuberculosis pathogenesis. *Pathogens and Disease* 76, (2018). <https://doi.org/10.1093/femspd/fty021> PMID: 29718271
7. Pandey K, A., Sassetti M, C. Mycobacterial persistence requires the utilization of host cholesterol. *Proceedings of the National Academy of Sciences of the United States of America* 105, 4376–4380 (2008). <https://doi.org/10.1073/pnas.0711159105> PMID: 18334639
8. Chang C, J., Miner D, M., Pandey K, A., Gill P, W., Harik S, N., Sassetti M, C. et al. igr Genes and Mycobacterium tuberculosis Cholesterol Metabolism. *Journal of Bacteriology* 191, 5232–5239 (2009). <https://doi.org/10.1128/JB.00452-09> PMID: 19542286
9. Nesbitt N, M., Yang X., Fontan P., Kolesnikova I., Smith I., Sampson S, N. et al. A thiolase of Mycobacterium tuberculosis is required for virulence and production of androstenedione and androstadienedione from cholesterol. *Infection and Immunity* 78, 275–282 (2010). <https://doi.org/10.1128/IAI.00893-09> PMID: 19822655
10. Yam C, K., D'Angelo I., Kalscheuer R., Zhu H., Wang X, J., Snieckus V. et al. Studies of a Ring-Cleaving Dioxygenase Illuminate the Role of Cholesterol Metabolism in the Pathogenesis of Mycobacterium tuberculosis. *PLoS Pathogens* 5, e1000344 (2009). <https://doi.org/10.1371/journal.ppat.1000344> PMID: 19300498
11. Hu Y., van der Geize R., Besra S, G., Gurcha S, S., Liu A., Rohde M. et al. 3-Ketosteroid 9alpha-hydroxylase is an essential factor in the pathogenesis of Mycobacterium tuberculosis. *Molecular Microbiology* 75, 107–121 (2010). <https://doi.org/10.1111/j.1365-2958.2009.06957.x> PMID: 19906176
12. Smith M, C., Baker E, R., Proulx K, M., Mishra B, B., Long E, J., Park S. et al., Host-pathogen genetic interactions underlie tuberculosis susceptibility. *bioRxiv* 2020.12.01.405514, (2021).
13. Aiewsakun P., Prombutara P., Siregar P, A, T., Laopanupong T., Kanjanasirirat P., Khumpanied T. et al. Transcriptional response to the host cell environment of a multidrug-resistant Mycobacterium tuberculosis clonal outbreak Beijing strain reveals its pathogenic features. *Scientific Reports* 11, 3199 (2021). <https://doi.org/10.1038/s41598-021-82905-x> PMID: 33542438
14. McDonough A, K., Rodriguez A. The myriad roles of cyclic AMP in microbial pathogens: from signal to sword. *Nature Reviews Microbiology* 10, 27–38 (2011). <https://doi.org/10.1038/nrmicro2688> PMID: 22080930
15. Chubukov V., Gerosa L., Kochanowski K., Sauer U. Coordination of microbial metabolism. *Nat Rev Microbiol* 12, 327–340 (2014). <https://doi.org/10.1038/nrmicro3238> PMID: 24658329
16. Molina-Quiroz C, R., Silva-Valenzuela C., Brewster J., Castro-Nallar E., Levy B, S., Camilli A. Cyclic AMP Regulates Bacterial Persistence through Repression of the Oxidative Stress Response and SOS-Dependent DNA Repair in Uropathogenic Escherichia coli. *mBio* 9, (2018). <https://doi.org/10.1128/mBio.02144-17> PMID: 29317513
17. Shenoy R, A., Visweswariah S, S. Mycobacterial adenylyl cyclases: biochemical diversity and structural plasticity. *FEBS Lett* 580, 3344–3352 (2006). <https://doi.org/10.1016/j.febslet.2006.05.034> PMID: 16730005
18. Tews I., Findeisen F., Sinning I., Schultz A., Schultz E, J., Linder U, J. The structure of a pH-sensing mycobacterial adenylyl cyclase holoenzyme. *Science* 308, 1020–1023 (2005). <https://doi.org/10.1126/science.1107642> PMID: 15890882
19. Townsend D, P., Holliday M, P., Fenyk S., Hess C, K., Gray A, M., Hodgson R, D. et al. Stimulation of mammalian G-protein-responsive adenylyl cyclases by carbon dioxide. *J Biol Chem* 284, 784–791 (2009). <https://doi.org/10.1074/jbc.M807239200> PMID: 19008230
20. Cann J, M., Hammer A., Zhou J., Kanacher T. A defined subset of adenylyl cyclases is regulated by bicarbonate ion. *J Biol Chem* 278, 35033–35038 (2003). <https://doi.org/10.1074/jbc.M303025200> PMID: 12829712

21. Abdel Motaal A., Tews I., Schultz E, J., Linder U, J., Fatty acid regulation of adenyl cyclase Rv2212 from Mycobacterium tuberculosis H37Rv. *FEBS J* 273, 4219–4228 (2006). <https://doi.org/10.1111/j.1742-4658.2006.05420.x> PMID: 16925585
22. Shenoy R, A., Sreenath P, N., Mahalingam M., Visweswariah S, S. Characterization of phylogenetically distant members of the adenylate cyclase family from mycobacteria: Rv1647 from Mycobacterium tuberculosis and its orthologue ML1399 from M. leprae. *The Biochemical journal* 387, 541–551 (2005). <https://doi.org/10.1042/BJ20041040> PMID: 15500449
23. Johnson M, R., McDonough A, K. Cyclic nucleotide signaling in Mycobacterium tuberculosis: an expanding repertoire. *Pathogens and Disease* 76, (2018).
24. Gazdik A, M., Bai G., Wu Y., McDonough A, K. Rv1675c (cmr) regulates intramacrophage and cyclic AMP-induced gene expression in Mycobacterium tuberculosis-complex mycobacteria. *Molecular microbiology* 71, 434–448 (2009). <https://doi.org/10.1111/j.1365-2958.2008.06541.x> PMID: 19040643
25. Bai G., McCue A, L., McDonough A, K. Characterization of Mycobacterium tuberculosis Rv3676 (CRPMt), a cyclic AMP receptor protein-like DNA binding protein. *J Bacteriol* 187, 7795–7804 (2005). <https://doi.org/10.1128/JB.187.22.7795-7804.2005> PMID: 16267303
26. Rickman L., Scott C., Hunt M, D., Hutchinson T., Menendez C, M., Whalan R. et al. A member of the cAMP receptor protein family of transcription regulators in Mycobacterium tuberculosis is required for virulence in mice and controls transcription of the rpfA gene coding for a resuscitation promoting factor. *Molecular microbiology* 56, 1274–1286 (2005). <https://doi.org/10.1111/j.1365-2958.2005.04609.x> PMID: 15882420
27. Rittershaus C, S, E., Baek H, S., Krieger V, I., Nelson J, S., Cheng S, Y., Nambi S. et al. A Lysine Acetyltransferase Contributes to the Metabolic Adaptation to Hypoxia in Mycobacterium tuberculosis. *Cell Chemical Biology* 25, 1495–1505 e1493 (2018). <https://doi.org/10.1016/j.chembiol.2018.09.009> PMID: 30318462
28. Nambi S., Gupta K., Bhattacharyya M., Ramakrishnan P., Ravikumar V., Siddiqui N. et al. Cyclic AMP-dependent protein lysine acylation in mycobacteria regulates fatty acid and propionate metabolism. *Journal of Biological Chemistry* 288, 14114–14124 (2013). <https://doi.org/10.1074/jbc.M113.463992> PMID: 23553634
29. VanderVen C, B., Fahey J, R., Lee W., Liu Y., Abramovitch B, R., Memmott C. et al. Novel inhibitors of cholesterol degradation in Mycobacterium tuberculosis reveal how the bacterium's metabolism is constrained by the intracellular environment. *PLoS Pathogens* 11, e1004679 (2015). <https://doi.org/10.1371/journal.ppat.1004679> PMID: 25675247
30. Guo L, Y., Seebacher T., Kurz U., Linder U, J., Schultz E, J. Adenyl cyclase Rv1625c of Mycobacterium tuberculosis: a progenitor of mammalian adenyl cyclases. *EMBO Journal* 20, 3667–3675 (2001). <https://doi.org/10.1093/emboj/20.14.3667> PMID: 11447108
31. Guo L, Y., U. Kurz A., Schultz A., Linder U, J., Dittrich D., Keller C. et al. Interaction of Rv1625c, a mycobacterial class IIIa adenyl cyclase, with a mammalian congener. *Molecular microbiology* 57, 667–677 (2005). <https://doi.org/10.1111/j.1365-2958.2005.04675.x> PMID: 16045612
32. Reddy K, S., Kamireddi M., Dhanireddy K., Young L., Davis A., Reddy T, P. Eukaryotic-like adenyl cyclases in Mycobacterium tuberculosis H37Rv: cloning and characterization. *Journal of Biological Chemistry* 276, 35141–35149 (2001). <https://doi.org/10.1074/jbc.M104108200> PMID: 11431477
33. Vercellino I., Rezabkova L., Olieric V., Polyhach Y., Weinert T., Kammerer A, et al R.. Role of the nucleotidyl cyclase helical domain in catalytically active dimer formation. *Proceedings of the National Academy of Sciences of the United States of America* 114, E9821–E9828 (2017). <https://doi.org/10.1073/pnas.1712621114> PMID: 29087332
34. Beltz S., Bassler J., Schultz E, J., Regulation by the quorum sensor from Vibrio indicates a receptor function for the membrane anchors of adenylate cyclases. *eLife* 5, (2016). <https://doi.org/10.7554/eLife.13098> PMID: 26920221
35. Ziegler M., Bassler J., Beltz S., Schultz A., Lupas N, A., Schultz J, E. Characterization of a novel signal transducer element intrinsic to class IIIa/b adenylate cyclases and guanylate cyclases. *FEBS Journal* 284, 1204–1217 (2017). <https://doi.org/10.1111/febs.14047> PMID: 28222489
36. Johnson M, R., Bai G., DeMott M, C., Banavali K, N., Montague R, C., Moon C. et al. McDonough, Chemical activation of adenyl cyclase Rv1625c inhibits growth of Mycobacterium tuberculosis on cholesterol and modulates intramacrophage signaling. *Molecular Microbiology* (2017). <https://doi.org/10.1111/mmi.13701> PMID: 28464471
37. Russell G, D., Huang L., VanderVen C, B. Immunometabolism at the interface between macrophages and pathogens. *Nature Reviews Immunology* 19, 291–304 (2019). <https://doi.org/10.1038/s41577-019-0124-9> PMID: 30679807

38. Nazarova V, E., Montague R, C., La T., Wilburn M, K., Sukumar N., Lee W. et al. Rv3723/LucA coordinates fatty acid and cholesterol uptake in Mycobacterium tuberculosis. *eLife* 6, (2017). <https://doi.org/10.7554/eLife.26969> PMID: 28708968
39. Gazdik A, M., McDonough A, K. Identification of cyclic AMP-regulated genes in Mycobacterium tuberculosis complex bacteria under low-oxygen conditions. *J Bacteriol* 187, 2681–2692 (2005). <https://doi.org/10.1128/JB.187.8.2681-2692.2005> PMID: 15805514
40. Griffin E, J., Pandey K, A., Gilmore A, S., Mizrahi V., McKinney D, J., Bertozzi R, C. et al. Cholesterol catabolism by Mycobacterium tuberculosis requires transcriptional and metabolic adaptations. *Chemistry & Biology* 19, 218–227 (2012). <https://doi.org/10.1016/j.chembiol.2011.12.016> PMID: 22365605
41. Baker J, J., Dechow J, S., Abramovitch B, R Acid Fasting: Modulation of Mycobacterium tuberculosis Metabolism at Acidic pH. *Trends Microbiol* 27, 942–953 (2019). <https://doi.org/10.1016/j.tim.2019.06.005> PMID: 31324436
42. Serafini A., Tan L., Horswell S., Howell S., Greenwood J, D., Hunt M, D. et al. Mycobacterium tuberculosis requires glyoxylate shunt and reverse methylcitrate cycle for lactate and pyruvate metabolism. *Molecular microbiology* 112, 1284–1307 (2019). <https://doi.org/10.1111/mmi.14362> PMID: 31389636
43. Akhter Y., Yellaboina S., Farhana A., Ranjan A., Ahmed N., Hasnain E, S. Genome scale portrait of cAMP-receptor protein (CRP) regulons in mycobacteria points to their role in pathogenesis. *Gene* 407, 148–158 (2008). <https://doi.org/10.1016/j.gene.2007.10.017> PMID: 18022770
44. Wells M, R., Jones M, C., Xi Z., Speer A., Danilchanka O., Doornbos S, K., et al. Discovery of a siderophore export system essential for virulence of Mycobacterium tuberculosis. *PLoS Pathog* 9, e1003120 (2013). <https://doi.org/10.1371/journal.ppat.1003120> PMID: 23431276
45. Griffin E, J., Gawronski D, J., DeJesus A, M., Ioerger R, T., Akerley J, B., Sassetti M, C. High-Resolution Phenotypic Profiling Defines Genes Essential for Mycobacterial Growth and Cholesterol Catabolism. *PLoS Pathog* 7, (2011). <https://doi.org/10.1371/journal.ppat.1002251> PMID: 21980284
46. Driver R, E., Ryan J, G., Hoff R, D., Irwin M, S., Basaraba J, R., Kramnik I. et al. Evaluation of a mouse model of necrotic granuloma formation using C3HeB/FeJ mice for testing of drugs against Mycobacterium tuberculosis. *Antimicrobial agents and chemotherapy* 56, 3181–3195 (2012). <https://doi.org/10.1128/AAC.00217-12> PMID: 22470120
47. Ji X, D., Yamashiro H, L., Chen J, K., Mukaida N., Kramnik I., Darwin H, K. et al. Type I interferon-driven susceptibility to Mycobacterium tuberculosis is mediated by IL-1Ra. *Nature microbiology* 4, 2128–2135 (2019). <https://doi.org/10.1038/s41564-019-0578-3> PMID: 31611644
48. Moreira-Teixeira L., Tabone O., Graham M, C., Singhanian A., Stavropoulos E., Redford S, P. et al. Mouse transcriptome reveals potential signatures of protection and pathogenesis in human tuberculosis. *Nature immunology* 21, 464–476 (2020). <https://doi.org/10.1038/s41590-020-0610-z> PMID: 32205882
49. Moreira-Teixeira L., Stimpson J, P., Stavropoulos E., Hadebe S., Chakravarty P., Ioannou M. et al. Type I IFN exacerbates disease in tuberculosis-susceptible mice by inducing neutrophil-mediated lung inflammation and NETosis. *Nat Commun* 11, 5566 (2020). <https://doi.org/10.1038/s41467-020-19412-6> PMID: 33149141
50. Lenaerts A., Barry 3rd, E, C., Dartois V. Heterogeneity in tuberculosis pathology, microenvironments and therapeutic responses. *Immunological Reviews* 264, 288–307 (2015). <https://doi.org/10.1111/imr.12252> PMID: 25703567
51. Bassler J., Schultz E, J., Lupas N, A. Adenylate cyclases: Receivers, transducers, and generators of signals. *Cellular Signaling* 46, 135–144 (2018).
52. Beites T., O'Brien K., Tiwari D., Engelhart A, C., Walters S., Andrews J. et al. Plasticity of the Mycobacterium tuberculosis respiratory chain and its impact on tuberculosis drug development. *Nature Communications* 10, 4970 (2019). <https://doi.org/10.1038/s41467-019-12956-2> PMID: 31672993
53. Warner D, F., Mizrahi V. Shortening treatment for tuberculosis—back to basics. *New England Journal of Medicine* 371, 1642–1643 (2014).
54. Zhang Y., Mitchison D. The curious characteristics of pyrazinamide: a review. *International Journal of Tuberculosis and Lung Disease* 7, 6–21 (2003). PMID: 12701830
55. Howard C, N., Khader A, S. Immunometabolism during Mycobacterium tuberculosis Infection. *Trends Microbiol* 28, 832–850 (2020). <https://doi.org/10.1016/j.tim.2020.04.010> PMID: 32409147
56. Pethe K., Sequeira C, P., Agarwalla S., Rhee K., Kuhen K., Phong Y, W. et al. A chemical genetic screen in Mycobacterium tuberculosis identifies carbon-source-dependent growth inhibitors devoid of in vivo efficacy. *Nature Communications* 1, 57 (2010). <https://doi.org/10.1038/ncomms1060> PMID: 20975714
57. Ganapathy U., J. Marrero J., Calhoun S., Eoh H., de Carvalho S, P, L., Rhee K. et al. Two enzymes with redundant fructose bisphosphatase activity sustain gluconeogenesis and virulence in Mycobacterium

tuberculosis. *Nature Communications* 6, 7912 (2015). <https://doi.org/10.1038/ncomms8912> PMID: [26258286](https://pubmed.ncbi.nlm.nih.gov/26258286/)

58. Crowe M, A., Casabon I., Brown L, K., Liu J., Lian J., Rogalski C, J. et al. Catabolism of the Last Two Steroid Rings in *Mycobacterium tuberculosis* and Other Bacteria. *mBio* 8, (2017). <https://doi.org/10.1128/mBio.00321-17> PMID: [28377529](https://pubmed.ncbi.nlm.nih.gov/28377529/)